Physical modelling of pore pressure development during impact pile driving using geo-centrifuge

MSc. Thesis

J.C.B. van Zeben

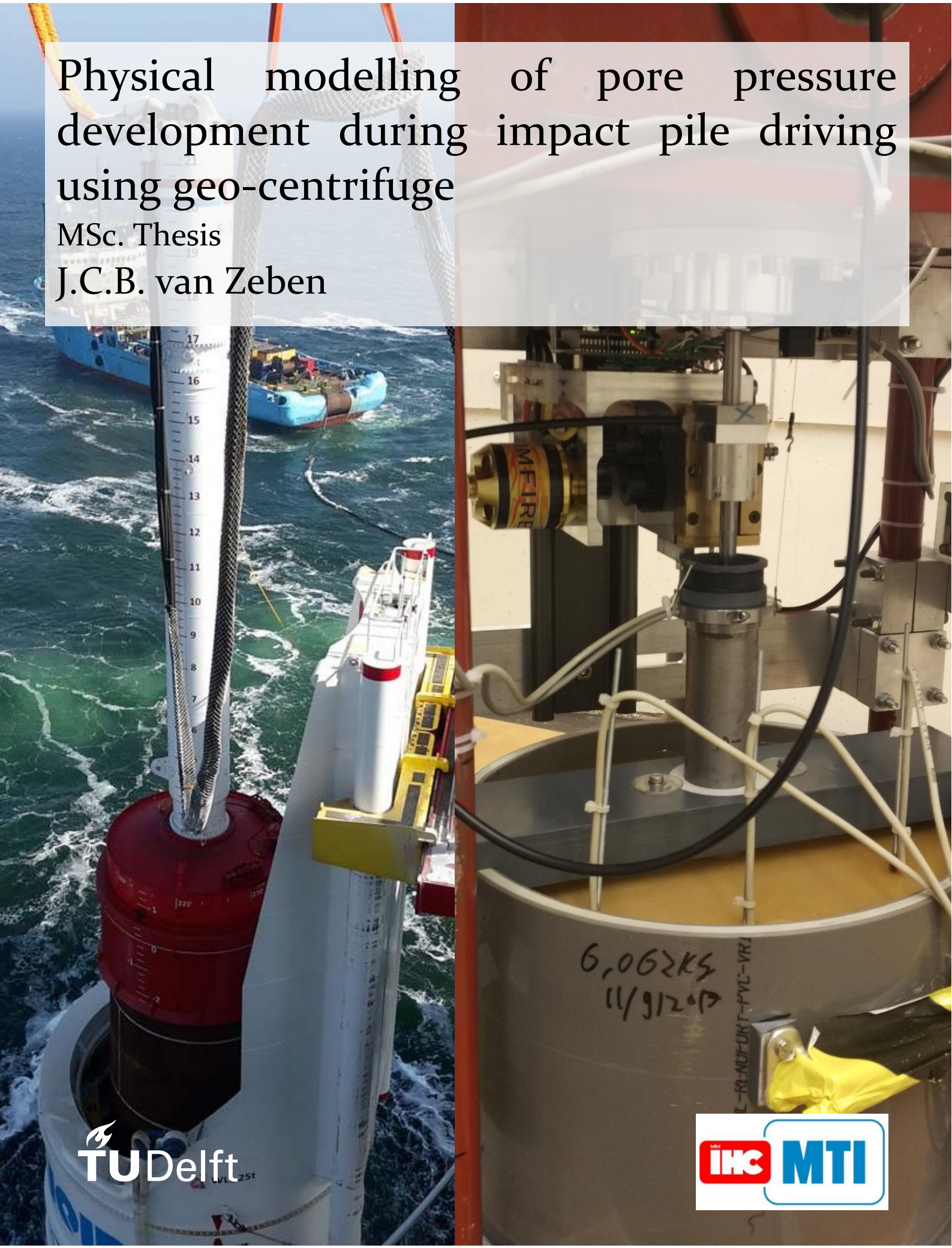

Physical modelling of pore pressure development during impact pile driving using geo-centrifuge

By

J.C.B. van Zeben

In partial fulfilment of the requirements for the degree of

Master of Science
In Applied Physics

At the Delft University of Technology
To be defended publicly on Thursday November 16, 2017 at 16:00 PM.

Supervisor:	Dr. A. Askarinejad	TU Delft
Thesis committee:	Prof. dr. K. Gavin,	TU Delft
	Dr. F. Pisano,	TU Delft
	Dr. Ir. M Alvarez Grima,	IHC MTI
	Dr. Ir. C. van 't Hof,	IHC IQIP

This thesis is confidential and cannot be made public until November 16, 2019

Preface

During this thesis I learned a lot. Not only were the skills and knowledge I acquired during my Master and my bachelor put to the test but also my determination and my perseverance. My main supervisor Amin Askarinejad came with this subject two weeks before I was leaving for a three month project in Nepal and quickly made me enthusiastic. During my Master the geo-centrifuge became the most interesting piece of equipment that the lab has. The chance of developing a new setup for the centrifuge sounded like a dream come true and would make an interesting and worthy end to a long time at the TU Delft. After an impromptu meeting with my supervisors from Royal IHC, Mario Alvarez Grima and Cornelis van 't Hof, my application for the thesis subject was approved and I could start 2 weeks after I came back from Nepal.

This thesis started with a lot of ambition. Not only was I making a new setup for the centrifuge but would also perform up to 20 tests and then perform secondary tests on an adapted setup using Particle Image Velocimetry. All this proved a bit much for one Master Thesis. The development of a new pile driving hammer took the better part of 10 months from concept to working setup and unfortunately took time away for doing extensive testing. Luckily my supervisors also see that and have ensured that research with my setup will continue. I am looking forward to see what comes out of future research.

Through the development of the setup I have learned a lot of mechanical and electrical engineering but also project management and the design process as a whole. I am glad I could experience this and was given the opportunity to do it. Because the development is such a large portion of the work I did, the depth I reached on the soil behaviour is less than I would have liked. There were a lot of highs and lows during my project and I have reached depths I did not know I had but I am glad I have them.

I would like to thank my committee for their support during this thesis. The almost weekly meetings we had were always very productive and helped a lot with the tasks ahead. I would also like to thank all the lab technicians that helped me to design and fabricate my setup. Mark, Jens, Arno, Karel, Leon, Bert, Paul, Fred and Martin were also there to answer questions and bounce ideas off. I would especially want to thank Han, Kees and Ron. Without them I would not have been able to finish this project. Furthermore I would like to thank Harry Bosch from DMC who provided glass fibre sensors I could use in the setup.

Furthermore I would like to thank all my fellow students and the staff members in the department. Without them this thesis would have been a lot less fun. Also all the discussions on my setup were very helpful especially when something broke, which at a certain point was almost a daily event.

Lastly I would like to thank my family. First my parents for always supporting me during my studies and giving me good advice when I needed it. My sister for giving me academic feedback on my work and some distractions when I needed them most. And of course my girlfriend Lilian for always being there for me even when I was very "knorrig".

Abstract

During the last decade, the focus of offshore activities have shifted from oil and gas production to offshore wind farm creation to reach the clean energy targets set by different nations. Foundation requirements for offshore structures have shifted because of this. The monolithic nature of windmills allows the use of a single open-ended steel pile as a foundation. While their installation procedure is similar to onshore piles, the dimensions of these open-ended piles are of a different scale, measuring up to 8 meters in diameter and 80 meters in length. The hydro mechanical response of the soil and the soil-structure interaction during the installation of the piles is complex and not yet fully understood. To better comprehend the soil behaviour during installation Royal IHC has initiated a research project in collaboration with the TU Delft. The current study is part of this research project. Using advanced physical and numerical modelling methods, a first step is made to gain better insight in the soil behaviour.

Using advanced physical centrifuge modelling techniques this study aims to provide insight into the soil behaviour and pile response during impact pile driving. The model can help validate numerical models and provide a controlled test environment for further modelling. To achieve this a new model impact pile driving setup was developed. This setup is capable of modelling the blow rate and impact energy of offshore pile driving hammers. A new data measurement system and sensor equipment was also created to capture parameters such as pore fluid pressure, blow rate, impact speed and pile displacement. Model piles can be installed in a controlled and repeatable environment. Special care has been taken to achieve correct coupling between the hydro mechanical response and the impact driving in the model.

Preliminary results from the model show no major scaling or modelling errors compared to numerical results. However validation of the model is needed and could be done by using a case study. The setup itself is operating efficiently and is highly adaptable for future research goals. The tests performed during this research were limited due to time constraints. Installation parameters such as pile displacement and pore fluid pressure development are in the range as expected. Furthermore, a correlation was seen between the radial distance from the pile tip and the increase of pore fluid pressure. Comparison of pile displacement with numerical models show similar results. Future studies should focus on varying impact pile driving parameters such as blow rate, blow energy and impact speed to define a correlation between the development of pore fluid pressure and impact pile driving parameters. This could improve the future efficiency of impact pile driving. The long term effects on the stability of the foundation should be regarded in future studies.

Contents

1 INTRODUCTION

1.1 OFFSHORE PILE DRIVING

During the last decade, the focus of offshore activities have shifted from oil and gas production to offshore wind farms creation. Foundation requirements for these two activities are distinctly different. Oil and gas structures are commonly built on jacket structures or large gravity based foundations. These techniques remain relevant for offshore windmills but the monolithic nature of windmills also allows for other foundation possibilities. The use of a single open-ended steel pile as a foundation has become common practice. While their installation procedure is similar to on shore piles, the dimensions of these open-ended piles are of a different scale, measuring up to 8 meters in diameter, 80 meters in length, with a wall thickness of 5 centimetres.

Several methods are available for the installation of these piles. The most commonly used methods are vibrating or hammering the pile. For vibrating, the entire pile needs to be excited, including the tip, to successfully install it. This can be difficult due to the length and size of the elements. This is less of an issue when using a pile driving hammer, as the main mechanism of installation is the concussive blow of the hammer block. This allows it to drive the pile through denser and stiffer soil layers.

During pile driving there is interaction between the soil and the pile along the interface. At the tip of the pile, displacement occurs as the pile moves down through the soil. Along the pile wall a shear force is exerted on the soil skeleton through friction during movement. These two mechanisms generate several soil responses, two of which are particularly interesting: Each blow of the hammer sends a compression wave through the pile. This wave also propagates through the soil. In combination with the movement of the pile, this puts extra strain on the soil skeleton and the pore fluid. In most conditions the hydraulic conductivity of the soil is not high enough to let this increase in pore water pressure dissipate before the next blow (Hwang et al, 2001). Consecutive blows will cause a gradual increase of the pore water pressure (Iskander, 2010). If the pore water pressure increases above the effective soil stress it will cause liquefaction in the soil. Liquefaction means that the soil loses all shear strength and starts behaving like a thick liquid. The process of liquefaction during pile driving continues to involve a lot of unknowns.

This thesis will investigate the soil behaviour that occurs during driving and can cause liquefaction. In order to investigate the mechanism, a pile driving hammer was developed for the TU Delft centrifuge. The design and development of this hammer will be explained in detail with respect to scaling and mechanical needs. The new pile driving hammer in combination with a high rate measurement system is also used to validate the numerical model created by (Azúa-Gonzalez C. , 2017). Several tests in both saturated and dry soil were done.

1.2 PROBLEM DESCRIPTION AND OBJECTIVE

The main objective of this research is to create a greater understanding of the pore water pressure development along open-ended piles during installation. To achieve this a new centrifuge test setup was developed for the centrifuge facilities at the TU Delft. The aim was to

perform two different kind of tests. First, the installation of open ended pile will be modelled. During the pile driving pore water pressures will be measured at different locations in the soil sample.

As there was no impact pile driving hammer setup available at the TU Delft centrifuge a significant part of the research consists of the design and development of a new pile driving hammer. This includes not only the pile driving hammer itself but also the instrumentation system needed to capture the desired parameters such as pile displacement, pore water pressure and blow energy.

The main objective of the research is to answer the following research question;

"How does pore water pressure develop during the installation of an open-ended pile during impact pile driving?"

1.3 Organization of Thesis

The remainder of this thesis is organized as follows: Chapter 2 provides an overview of current research on impact pile driving and soil structure interaction during pile installation. Chapter 3 details centrifuge modelling and model scaling in the increased gravity field. The design and development of the pile driving hammer for the TU Delft centrifuge is explained in detail. The development of the instrumentation in the setup is also discussed in this chapter. Finally, the sample preparation method is reviewed. Chapter 4 gives an overview on the tests performed with the pile driving hammer setup. An analysis is presented of the data and a comparison between of the results is made. Chapter 5 presents conclusions from the research, followed by recommendations on both the experimental setup as well as future test possibilities.

2 PORE FLUID PRESSURE DEVELOPMENT DURING IMPACT PILE DRIVING

Impact driving of a foundation pile is done by striking the top of the pile with the ram mass of the pile driving hammer. A pile can be made out of different materials but most commonly either steel or concrete is used. These piles can differ in length and cross section depending on the needs of the foundation. For onshore foundations prefabricated concrete piles are often used. They are made to specification and foundation requirements for onshore structures fall within the bearing capacity of these piles. Because of limitations to the hammer from noise restrictions and vibrations to surroundings onshore piles are often not larger than 500*500 mm^2. Making the pile larger would require a heavier hammer to reach the target depth. When looking to offshore structures the requirements change. Offshore structures experience higher dynamic loads than most onshore structures as they have loading from waves and wind. The increase in loading combined with the more aggressive environment off shore means steel foundation piles are most often used. The size of these foundation elements are also of a different dimension. Offshore structures can be very large and can require large foundation piles. Because the location is offshore where noise and vibration restrictions are lower due to the lack of direct surroundings. Larger piles can be used and also stronger hammers. In the last years the sizes of the foundation elements has grown significantly as the demand of offshore wind turbines has increased. These turbines are often placed on a single foundation pile with a diameter of up to 8 meters and lengths that can reach 80 meters. Because a full displacement pile would not be able to reach the required depth these piles are open ended with a wall thickness in the range of 5 to 10 cm.

During the impact driving of these large foundation piles several things are happening in the soil. This thesis will mainly investigate the pore water pressure development. Connected to the pore water pressure development is the shear band development which will also be investigated.

2.1 PORE PRESSURE DEVELOPMENT

Soil behaviour is very complex and difficult to model because the behaviour is governed by the interaction between a solid and a liquid. Soil and especially in offshore conditions is a combination of solid soil particles aligned in a soil skeleton with the voids in between the particles filled with a pore fluid. In most cases this is water but it can also be a contaminant or a gas. During impact pile driving the pore fluid pressure, PFP, is loaded in two distinct ways.

Firstly when the pile is struck by the ram mass of the impact pile driving hammer a compression wave moves through the pile. When the wave reaches the toe of the pile the compression wave is transmitted into the soil. A tension wave also propagates back-up in the pile. The compression wave that is exerted on the soil propagates through the soil with a spherical wave front while vertical shear waves propagate in a conical wave front from the shaft friction on the pile (Attewel & Farmer, 1973). The waves propagating from the pile can cause an increase in PFP which depending on the soil and soil layering can either quickly dissipate or build up. Generated PFP can dissipate quickly in high permeable soils such as sand whereas PFP cannot dissipate fast enough in impermeable soils such as clay.

Secondly the soil is deformed due to the movement of the pile. The continued driving of the pile induces cyclic loading on the soil causing deformation. The movement of the pile compacts the soil directly under the toe of the pile and compresses the soil around the pile. The mechanism of shearing due to the shear stresses exerted from the pile wall and also the compaction under the pile tip depends on two parameters, the relative density and the hydraulic conductivity. Depending on the relative density of the soil the shear stresses exerted from the pile wall can cause compaction or dilation of the soil skeleton. Secondly the hydraulic conductivity of the soil affects if the loading is under drained or, partially, undrained condition. Under drained condition means that a change in pore pressure can dissipate during the loading. In undrained loading the change in pore pressure cannot dissipate quickly enough during the loading resulting in an increase in pore pressure. The stress state of a soil is governed by the following equation where σ is the total vertical stress, σ' is the effective vertical stress and p is the pore fluid pressure.

$$\sigma = \sigma' + p$$

In an undrained condition where the pore pressure goes up under constant loading there is a reduction in effective stress. Effective stress in this formula indicates the stress between grain particles. When effective stress goes to zero the soil grains no longer exert any force and loses the capability to transfer any shear strength and the soil liquefies. During pile driving the blow rate is normally so high that it can be seen as a partially undrained condition. PFP increases during pile driving, even if it is a single blow. The high blow rate causes accumulation of excess PFP because the excess PFP cannot dissipate quickly enough. This can eventually result in enough excess PFP to cause liquefaction. As can be seen in Figure 1 the effects on the soil are different depending on the soil density. In a loose soil which has the tendency to contract during loading. This causes a reduction in void ratio and temporarily a reduction in strength due to the increase of PFP. In a dense sand the soil skeleton is prevented from dilation due to the undrained conditions. This causes a reduction in PFP due to the inability for the pore fluid to flow into the new voids created quickly enough. This can temporarily increase the strength of the soil.

During pile driving the combination of the wave propagation through the soil and the deformation of the soil can have a significant effect on the PFP. If this can cause liquefaction and thus complete loss of shear strength in the soil and how this is related to impact pile driving is yet to be determined.

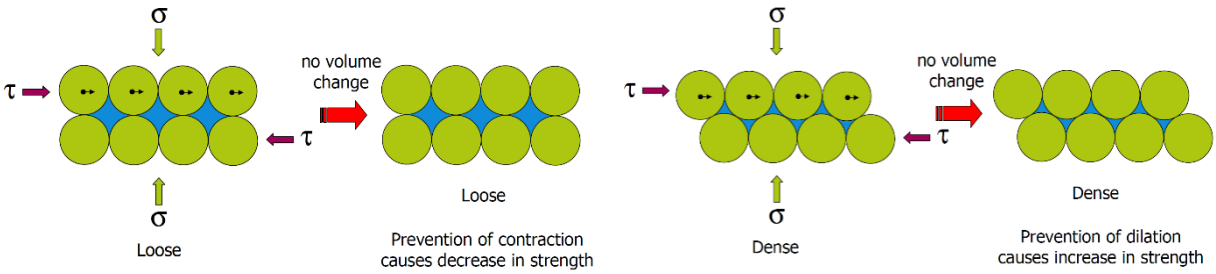

Figure 1 Undrained shear mechanism. Adapted from (Hicks. M.A., 2015)

2.2 STRESS STATES DURING PILE INSTALLATION

As stated in the previous section the shear stress exerted on the soil has an influence on the PFP during, partially, undrained loading. When a pile is driven the soil experiences several different loading scenarios. When looking at a soil element in the path of the, to be installed, pile several stress stages can be defined (White D. , 2005). These stages are shown in Figure 2. As the pile tip approaches the soil element the stresses on the element is increased and it is pushed laterally to finally pass the pile. As the pile tip passes the soil element, the stress level is decreased and the element can exert an upward shear stress on the pile. At this point the maximum shear stress is exerted on the pile. As the pile penetrates deeper the soil element comes under cyclic loading from the pile driving. The repetitive loading from the pile wall causes gradual densification of the soil at the pile surface (White & Bolton, 2002). This densification causes an effect called friction fatigue which describes the decrease of horizontal stress acting on the pile wall with increased penetration (Heerema, 1980). For this research the stages A until D in Figure 2 are of interest as this is the focus of the centrifuge model. The pile displacement and change in stresses

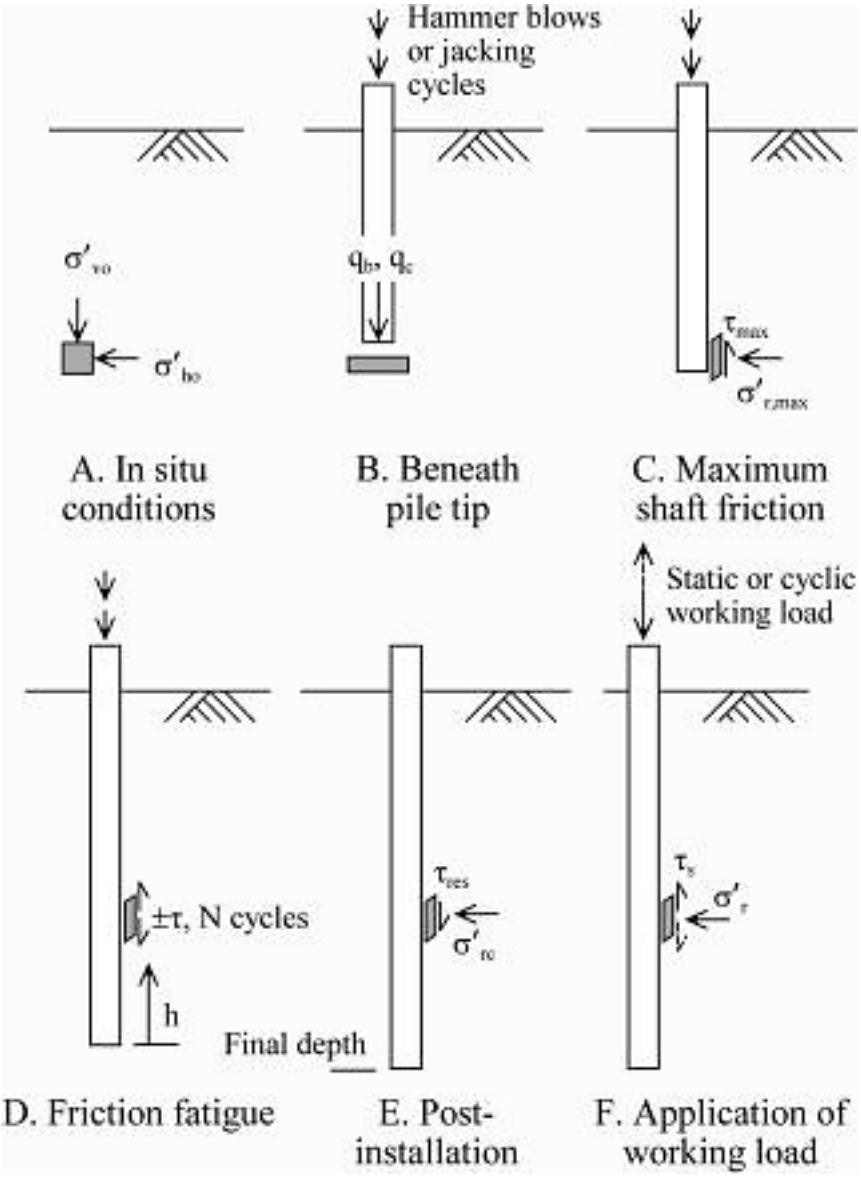

Figure 2 Stages in the loading history of a soil element adjacent to a displacement pile (White, 2005)

exerted on the soil elements as the pile is driven in the soil are the main causes of pore pressure development resulting from shear forces.

2.3 CONCLUSION

The soil mechanisms described in this chapter form the basis of the research performed. The influence of wave propagation and shear stresses on pore fluid pressure have long been acknowledged and also extensively researched. The addition the current research wants to make to this field is a deeper understanding of the influence of impact pile driving on this development of pore fluid pressure. Especially how different blow rates and blow energy can influence it and if it can help improve the efficiency with which piles are installed. If the soil around a pile is liquefied installation can perhaps be done faster and with less energy. Since the demand of these foundation piles will continue to go up this can help reduce installation time and costs.

3 CENTRIFUGE MODELLING

This section discusses centrifuge modelling, specifically, subsection 3.1 outlines the scaling laws governing centrifuge research and how they affect the model properties; subsection 3.2 sets out the experimental setup developed for this thesis; subsection 3.3 details the sample preparation used to prepare the soil samples; and finally, subsection 3.4 discusses the experimental setup.

3.1 SCALING LAWS AND EFFECTS

3.1.1 Scaling laws

Experimental research in geo-engineering can take three forms: small scale tests under 1 g; full scale tests; and, small scale tests under higher g level. As soil behaviour is stress dependent, small scale testing under 1 g is not always suitable to model behaviour. In these cases, full scale tests enable proper modelling of the problem but require considerable resources. Centrifuge tests are a cost-effective method of conducting accurate small scale modelling. Because of the increased gravity field the stress condition of the soil is similar to that of a full scale model. This is the major disadvantage of small scale tests under 1 g as soil behaviour has a non-linear stress-strain relationship (Klinkvort & Hededal, 2010) (Askarinejad, et al., 2012). As the gravity field is increased, it is important to properly scale the various elements of the model. Extensive research has been performed regarding scaling laws (Garnier, et al., 2007). For this research centrifuge test was chosen as an appropriate way to model pile behaviour.

Parameter	Scaling factor (model/prototype)
Acceleration	N
Linear dimension	1 / N
Stress	1
Strain	1
Mass	$1 / N^3$
Unit weight	N
Force	$1 / N^2$
Energy	$1 / N^3$
Impulse	$1 / N^3$
Frequency	N
Velocity	1
Dynamic time	1 / N
Seepage time	$1 / N^2$

Table 1 Scaling laws

The prototype system needs to be scaled down to model system size. The geometry and other aspects of the prototype are scaled using the factor N. N is the factor by which the gravity field is increased. A significant amount of research has been done in this field and for most parameters a proper formulation has been made between prototype and model dimensions. The International Journal of Physical Modelling in Geotechnics 3 has gathered these laws into one document, (Garnier, et al., 2007), not all of which are relevant to the current research. Table 1 provides a short overview of the parameters that are applicable to this research.

An important factor to consider when modelling a dynamic event in the centrifuge is the coupling of a dynamic event such as pile driving and the seepage or dissipation of pore fluid pressures. The impact pile driving is a dynamic event that has a scaling factor of 1/N. However the dissipation of pore fluid pressure or consolidation has a scaling factor of $1/N^2$. As these two processes are coupled in the model this causes an issue. The consolidation process is governed by two main equations (Askarinejad et al, 2017). First the volume flow per unit time is derived from Darcy's law.

$$\frac{\Delta V}{t} = k * i * A * t$$

Where *k* is the permeability, *i* the hydraulic gradient and *A* the area of porous media. The change in volume is associated with this flow volume due to stress change in the porous media (Wood, 2003). This volume change is dependent on volumetric strain rates and the initial volume.

$$\Delta V = \epsilon * V_{init}$$

From (Taylor, 1948) and (Wood, 2003) the scaling factor for these two volumetric changes can be found to be

$$\frac{N}{N_\mu}\frac{N_\rho}{N_{\rho f}} N_{ts} N_l^2 = N_l^3 \frac{N_\rho N N_l}{N_G}$$

For the seepage time scaling N_{ts} this gives a scaling factor of $1/N^2$ if the viscosity of the pore fluid and the soil stiffness is scaled with a factor of 1. This means that if water is used as a pore fluid in the model the two processes will not be coupled properly. To model the soil behaviour it is necessary to decrease the consolidation duration by a factor N. This can be done by either decreasing the permeability of the soil or by increasing the viscosity of the pore fluid. Decreasing the permeability of the soil can be difficult and possibly affects other soil parameters such as grain size, stiffness and strength. Also, this would have a limited effect in this research as changing the permeability of the soil is predominantly done by using a smaller grain size for the sample soil (Kutter, 1992). The sand chosen for the current research is a very fine and if decreased further would no longer be classified as sand. Therefore it is easier to change the viscosity of the pore fluid (Askarinejad et al, 2015 & 2017). Several possible pore fluids have been developed in the past to achieve this such as silicon oil (Haigh & Madabhushi, 2002) and glycerin mixture (Askarinejad et al. 2015). For this research the viscous fluid developed by Deltares (Allard & Schenkeveld , 1994) will be used. This fluid is a water based mixture with a thickening agent. The viscosity of the fluid is 51.89 cSt at 20° Celsius. As the viscosity of the fluid is temperature dependent and the centrifuge room is relatively warm this ensures the correct viscosity during testing.

3.1.2 Gravity curve and effect

The gravity level or g level, created within the centrifuge is dependent on two main parameters, the rotational velocity and the radius from the rotational axis. The relationship between the scaling factor *N*, gravitational acceleration *g*, the rotational speed ω and the radius *r* from the axis is given by the following formula and visualized in Figure 4 and Figure 3.

$$Ng = \omega^2 * r$$

As the radius from the axis dictates the g level it varies over the depth of the soil sample. This means that the stress level is correctly scaled at one level in the soil sample. Above and below

this level the stress level is respectively lower and higher than the intended stress level. Because of this gradient in g level a centrifuge with a larger radius can be beneficial as the radius factor has less influence. Because the TU Delft centrifuge is relatively small with a 1.22 m radius, there is a considerable gradient along the centrifuge carriage which is 550 mm tall. For this research the g level during testing is defined at the middle of the expected depth of pile displacement. At that depth the most important soil behaviour occurs and stresses at this level are most crucial. The g level gradient is important to keep in mind during the design of the pile driving hammer. If the ram mass accelerates under free fall is it subject to the g level gradient during free fall. This should be considered when calculating fall time, fall height and impact speed.

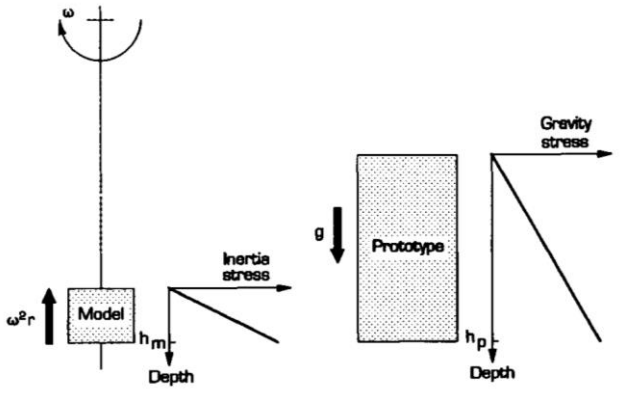

Figure 4 Inertial stresses in a centrifuge model induced by rotation about a fixed axis correspond to gravitational stresses in the corresponding prototype (Taylor. R.1995)

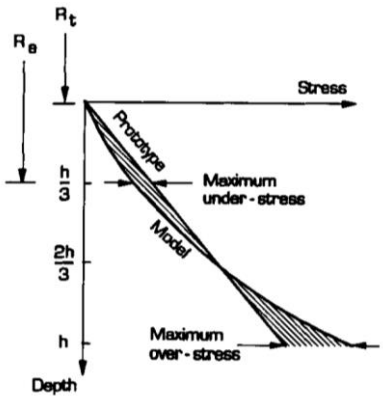

Figure 3 Comparison of stress variation with depth in a centrifuge model and its corresponding prototype (Taylor. R. 1995)

3.1.3 Particle size

Grain size is not directly scaled in the soil sample during centrifuge testing. As soil behavior is related to particle size, scaling the particle size would mean that a fine sand at prototype level would scale down to a clay at model level. To ensure similar mechanical properties of the soil between prototype and model, similar soil is generally chosen (Bolton & Lau, 1988). For the current research a fine GEBA sand was chosen. This sand has a very narrow grain size distribution between 0.080 and 0.200 mm and consists for 99% out of silica. It has been frequently used before at TU Delft and the soil parameters were extensively determined (Krapfenbauer, 2016).

Table 2 gives an overview of the soil properties. The mechanical properties of the sand also showed similarity with installation locations of Royal IHC. If wanted this makes it possible to compare the results from this research to these tests in the future.

The grain size was an important factor in the choice of sand. The soil structure interaction at the basis of the soil mechanism as stated in the previous chapter needs to be properly scaled. Firstly the interaction between the pile and the soil needs to have a specific ratio between the wall thickness *t* and average grain size. If the grains are relatively large in respect to the wall thickness *t* the amount of grains under the pile is insufficient to properly model the soil behaviour. According to (De Blaeij, 2013), (Garnier, et al., 2007) and (De Nicola & Randolph, 1997) the t/D50 should be at least 10 and preferably above 15. Furthermore the thickness of the shear band that develops along the pile is dependent on the average grain size. The thickness of the shear band is typically between 10-15 times the average grain size (Garnier & König, 1998)

(Muir Wood, 2004). As the grain size is not fully scaled in centrifuge tests the shear band thickness in the model would become much larger than in the prototype. To reduce this scale effect the ratio between the outer pile diameter D_0 and the D_{50} should be larger than 100 (Dijkstra, 2009). These ratios between the grain size and dimensions of the pile should be adhered during the design choices of the centrifuge model.

Property	Symbol		Unit
Specific Gravity	γs	2650	[kg/m3]
Average grain size	D_{50}	0.103	mm
Lower 10% grain size	D_{10}	0.90	mm
Lower 60% grain size	D_{60}	0.110	mm
Maximum void ratio	e_{max}	0.934	[-]
Minimum void ratio	e_{min}	0.596	[-]
Coefficient of curvature	Cc	1.47	[-]
Coefficient of uniformity	Cu	1.22	[-]
Angularity		Rounded-Subangular	[-]
Critical state friction angle	Φ_{cs}	30±1	[o]

Table 2 Fine GEBA sand properties (Krapfenbauer, 2016)

3.1.4 Boundary conditions

Boundary conditions can influence model behaviour. As the boundary created by the sample container creates a hard boundary for both soil behaviour as well as wave propagation. To mitigate these effects as much as possible the largest possible container was constructed for the TU Delft centrifuge. Previous research showed that the boundary should be at least 6 pile diameters for open ended pile installation (De Nicola, 1996). This would be problematic as even in the largest container it would be impossible to have a model pile of a dimension desired for this research. To further understand the boundary conditions in the container and their effects on the soil behaviour numerical simulations of the model setup were done (Azúa-Gonzalez et al, 2017). The numerical simulations were done with both a hard boundary and a soft viscous boundary to simulate a free boundary condition. The numerical simulations showed that the boundary does have an effect and that it is also dependent on the relative density of the soil and the drainage conditions. For a dense sample with nearly undrained conditions the boundary conditions have the largest influence. This effect is less profound with a loose sample under drained conditions. The difference however between these limit states on pile displacement and pore pressure development was less than 10% when testing at 30g. Under 50g the influence from the boundaries was even less on pile displacement and pore pressure development because of the increased prototype geometry and increased stresses. These numerical simulations indicate that even though there are some boundary effects from the container the magnitude is not of such a degree that it greatly influences the soil behaviour. On the basis of this conclusion three sample containers with an internal diameter of 295 mm were constructed.

3.2 CENTRIFUGE SETUP

The experimental setup consists of two main parts, the pile driving hammer system and the instrumentation system. This section will go into detail of the design process of both systems.

3.2.1 Pile driving hammer

Previously a small pile driving device was created for the TU Delft centrifuge to hammer piles with a diameter of 15 mm using a pneumatic system. This system has since then been decommissioned. Moreover the system was designed to drive smaller piles at a lower blow rate than needed for this research. Therefore a new pile driving device needed to be designed to accommodate the current research's need for a system that could drive large diameter open ended piles with the required blow rate and blow energy. A literature re-view of current hammer devices, such as the pneumatic system described by (De Nicola & Randolph, 1994) and other systems as described by (Levancher et al, 2008), showed that various systems have been successfully developed in the past. An overview of centrifuge pile drivers is given in Table 3.

Date	Origin	Type of pile driver	Ram mass [g]	Free fall [mm]	Frequency [Hz]
1988	Cambridge (UK)	Pneumatic jacket	95	62	2.5
1991	Boulder Univ. (USA)	Pneumatic	170	50	27.7
1994	UWA (Australia)	Pneumatic	70	0-20	0-20
1994	LCPC (France)	Electromagnet	163.8	0-32	1/6
2008	LCPC (France)	Electromagnet	70	24	-

Table 3 Overview of centrifuge pile driving hammers

For the development of the new pile driving hammer two main aspects were guiding. Firstly the blow rate of the prototype hammers needed to be scaled correctly. The prototype pile driving hammers were the IHC Hydrohammer S series; specifically the Hydrohammer S200, S280 and S500 with a blow rate of ca. 45 blows per minute. Secondly the blow energy from these prototype hammers needed to be scaled correctly. The hammers are capable of delivering a blow energy between 20 and 500 kJoule.

The maximum impact speed that these hammers can achieve is 6.3 m/s. As the blow energy is a function of the ram mass and the impact speed, 6.3 m/s was taken as the basis for the determination of the required ram mass. From this basis an analysis was made of the required fall height, lift speed and ram mass for different g levels. This was combined with the limitations regarding the prototype pile with respect to boundary conditions and scaling effects. This analysis showed that 50g was optimal for the model. A lower g level would be unable to scale the desired prototype pile while a higher g level proved problematic regarding lift speed and blow rate. At 50g a blow rate of 35 Hz would be required and a ram mass between 110 and 240 grams to achieve the desired blow energy at 6.3 m/s impact speed.

After the determination of the g level and on the basis of previous designs from literature three main systems were investigated to perform the lift. A pneumatic system, an electrical magnetic system and an electrical mechanical system were all investigated in a concept design. The

pneumatic system proved problematic due to the cycle time of pneumatic valves and the required pressures to lift the ram mass. The electrical magnetic system had an advantage of strong pull force but the stroke required to achieve the correct impact speed would be problematic. This combined with a complex fabrication process disqualified it. The electrical mechanical system was most feasible. The fabrication of the system was least complex and showed great adaptability for future needs. Parameters such as fall height, blow rate and ram mass can all easily be adapted in this design.

The basis of the lift mechanism is a flywheel that picks up the ram mass at its lowest point and releases it at a predefined point. From this point the ram mass accelerates under free fall. As the ram mass strikes the anvil the pile is driven into the soil. Following the strike on the anvil the pile driving hammer moves down towards the pile to keep the fall height constant. The ram mass is subsequently lifted again and the process repeats.

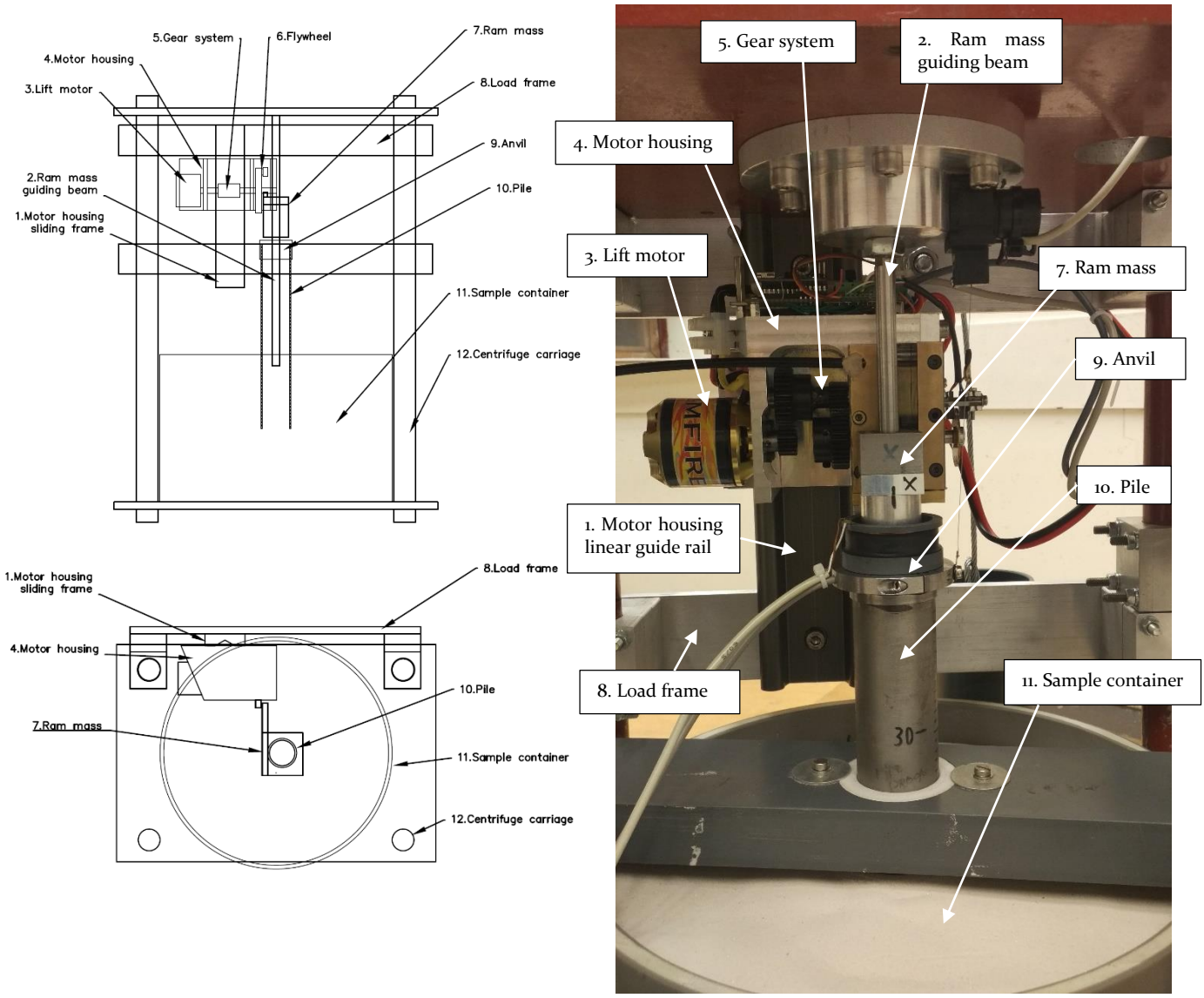

Figure 5 Overview Pile driving hammer

The test procedure starts with the ram mass locked in place by the ram mass release mechanism. This is a pin that locks the ram mass above the path of the flywheel. Testing starts with spinning up the centrifuge to the desired g level. After this has been reached and the model has stabilized under the increased g level the flywheel is activated and accelerated to the RPM corresponding to the desired blow rate. The release pin is withdrawn and the ram mass is released in the path of the flywheel starting the pile driving. For single blow pile driving the test procedure is similar except that the flywheel is not activated. Care needs to be taken that the notch on the flywheel is out of the path of the ram mass as it will interfere with the free fall.

The pile driving setup consists out of three main elements: the pile driving hammer, the ram mass system, and the pile-anvil system. The pile driving hammer includes the motor housing, the load frame, ram mass release mechanism and the counterweight. The ram mass system includes the ram mass, the ram mass guiding beam and the guiding beam fixation. The pile system includes the pile, the pile cap, the motor-pile connection and the pile guide. A schematic overview is given in Figure 5. These systems will be explained in detail in the following sections. A complete set of technical drawings of the setup can be found in Appendix B.

Pile driving hammer system

At 50g a model blow rate of ca. 35 blows per second is required. The prototype hammers are commonly used as offshore pile driving hammers with a ram mass larger than those of onshore hammers. The prototype hammers deliver a blow energy between 20 and 500 kJoule. To achieve the correct scaled energy per blow a relatively heavy ram mass was needed. Scaling laws showed that a ram mass between 110 and 240 grams, was needed to be able to achieve the blow energy needed at a maximum impact speed of 6.3 m/s. While the hammer is designed for 50g functionality the acceleration of the ram mass is lower. This is due to it being closer to the axis of rotation. The 50g acceleration level is set at the middle of the soil sample. The g-level at the starting position of the ram mass is ca. 38g. At this g level it will take the ram mass 16 milliseconds to reach the desired 6.3 m/s impact speed. This can be achieved over a distance of 50 mm. As the pile is driven deeper into the soil the fall time and fall distance will decrease to achieve the desired fall speed. This change is not significant enough to be included in the design. The total fall time per second, on the basis of a fall time of 16 milliseconds and a blow rate of 35 Hz, is 560 milliseconds. Per second this leaves 440 milliseconds to lift the ram mass back to its top position. One complete cycle of falling, transferring energy to the pile system and lifting the ram mass can take a maximum of 28 milliseconds. The mechanism that lifts the ram mass has less than 12 milliseconds to perform the 50 mm lift.

The basis of the electrical mechanical system is a flywheel with a notch that connects to a pin on the ram mass. The notch is constructed from an 8 mm stainless steel pin with a rotary ball bearing at the end. The ball bearing reduces the friction between the notch and the pin as the flywheel rotates. The notch is bolted into a hole on the flywheel and secured with Loctite. The flywheel has been balanced to counteract the unbalance resulting from the added mass of the notch. If not balanced the flywheel creates significant vibrations. The fall height can be adapted by decreasing the distance between the flywheel and the anvil. The flywheel is powered by an electric motor. The inertia helps lift the ram mass decreasing the shock to the system and the needed response time of the electric motor. During one blow cycle the flywheel does one

rotation which at a 35 Hz blow rate takes 28 milliseconds. This equals a RPM of 2100 for the flywheel. Within the 28 milliseconds of one revolution 16 milliseconds is for the fall of the ram mass. In this time the flywheel has rotated 206 degrees since release of the ram mass and leaving 154 degrees for lifting the ram mass. To achieve this a diameter of 76 mm for the flywheel was chosen. The lift notch is located 29.5 mm centre to centre distance from the axis of the flywheel. This diameter makes it possible to achieve the required lift of 50 mm within 120 degrees of the flywheel. This leaves a margin for transferring the energy into the pile and any delays due to friction on the ram mass. Secondly the electric motors rotational speed increases slightly after the release of the ram mass due to the loss of the extra load on the flywheel. The acceleration is counteracted by the slight decrease in rotational speed as it lifts the ram mass. Combined with a RPM sensor the rotational speed is kept constant during driving.

The maximum power the electric motor needs to supply is governed by the force required to lift the heaviest ram mass of 240 grams. At 50g simulation the ram mass weighs a maximum of 100 N. The momentum created by the ram mass on the axis of the flywheel through the notch is 3 Nm. The power requirement at 2100 RPM to create this minimum momentum on the wheel is 660 Watt. While electric motors can provide high torque at low RPMs they still have a linear increase until optimal RPM is reached. Achieving the needed torque from standstill was not possible with the available electric motor models and the space requirements. To mitigate this the motor first needs to spin up to the desired RPMs after which the ram mass is released in the path of the flywheel and the lift notch. This way the motor is running at peak performance and does not need to provide the required power from standstill. The Rimfire 1.20 by Electrifly was chosen to power the hammer. This 1.2 kW outrunner brushless motor with a peak burst power of 2.3 kW provides a wide margin for the power requirement. The size of the motor, with a diameter of 50 mm and a length of 65 mm, makes it easy to fit in the centrifuge setup. The electric motor is controlled by a Wasabi Eco 35A controller by Yuki. The electric motor is not powered by the built in 5V power supply of the centrifuge as it has a much higher power requirement. A 6 cell 14.8V 1300 mA LiPo battery provides power to the electric motor. Both the flywheel and motor axle are located on rotary ball bearings. To prevent alignment issues between the bearings initially a flexible beam coupling was initially used to connect the motor and the flywheel.

The motor housing houses the flywheel and the motor. Figure 6 shows a section view of the motor housing. The motor housing is milled out of a single piece of aluminium to keep the mass low. It has a detachable plate on one side to mount the flywheel. The entire motor housing is connected with a linear guide rail by IGUS to the load frame to allow it to follow the pile as it is driven. This ensures that distance from the pile anvil, and thus fall height, is kept constant. The motor housing is connected with a vibration free pinhole connection on the pile anvil. As the motor housing - including the flywheel, gears and electric motor - weighs ca. 3 kg, a stiff connection would put a disproportional load onto the pile. Therefore a counterweight was connected to the back of the motor housing via a cable and pulley system. An IGUS W-16-60 linear guide rail was used to mount the motor block and provide vertical movement. As the pile penetrates the soil, the motor housing follows it downwards. The g-level is dependent on the distance from the axis of the centrifuge. As the motor housing moves away from the centrifuge axis and the counterweight moves towards the axis, resulting in a change in the balance between

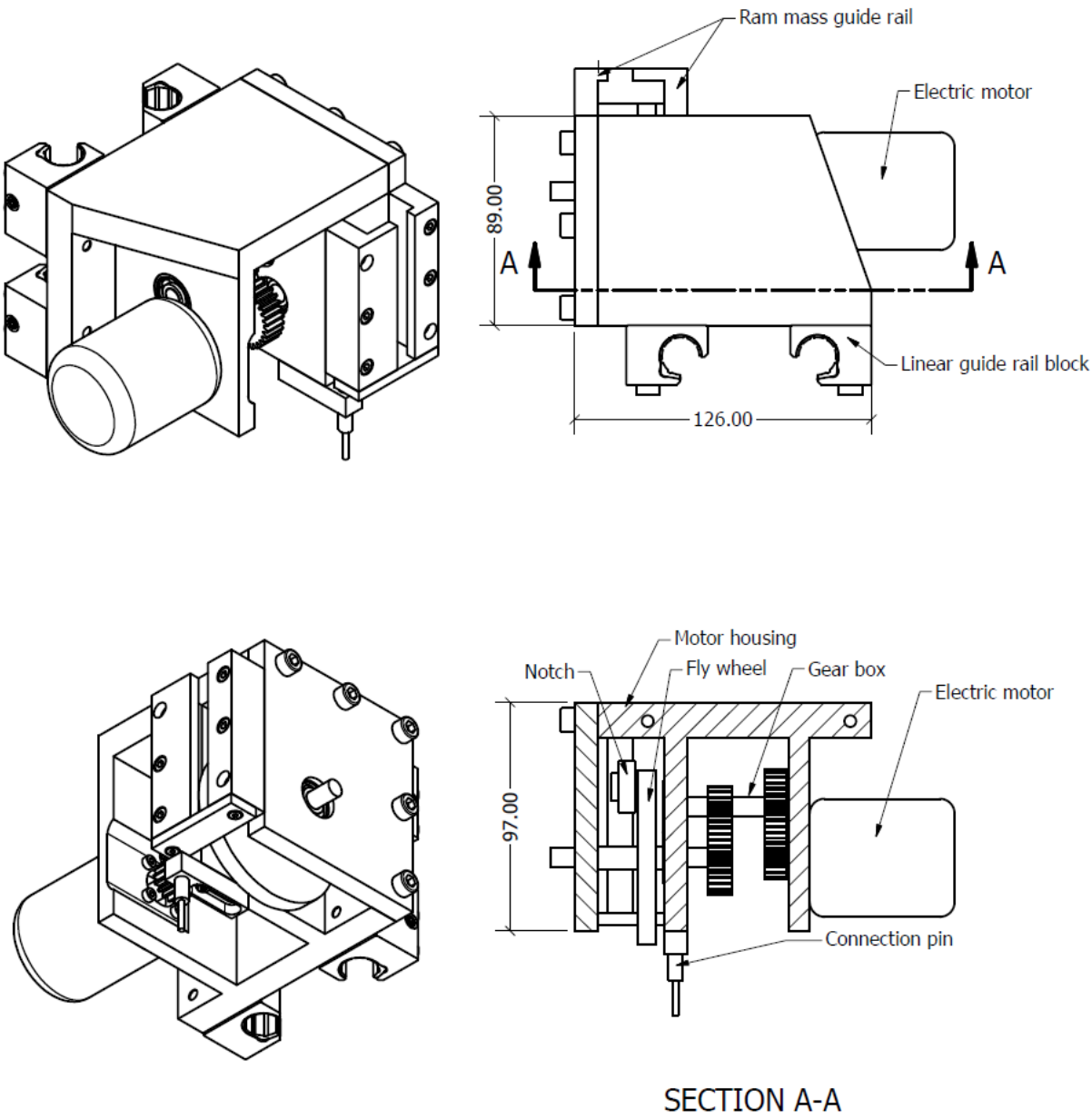

Figure 6 Detailed view of motor housing. Dimensions in mm

these two components. To counteract this, a spring is connected to the motor housing that comes under tension as the motor housing moves down. This spring compensates the unbalance resulting from the changing g-level. The system is balanced in such a way that the motor housing is always pressing very slightly on the pile and has a resulting force downwards. The extra load from lifting the ram mass is also transferred to the pile through the connection between motor housing and pile anvil. In practice, the load of the hammer and the resulting force from lifting the ram mass are also transferred into the pile and not into the piling rig.

The ram mass release mechanism is attached to the ram mass guide rail in front of the flywheel. This guide rail is in place to keep the ram mass from rotating and misalign with the flywheel. The guide rail is made out of red brass to minimize friction. The bottom of the guide rail is closed to prevent the ram mass from falling to low. If the ram mass falls to low it moves out of the path of the flywheel and can seriously damage the pile driving hammer. The release pin is made out

of a 2 mm steel cable with a hard soldered end to provide rigidity and situated in a rigid outer lining. The cable is fed through a hole in the guiding rail. The cable is retracted by a LF-20MG servo by Power HD with a torque of 20kg-cm. A previous iteration of this mechanism with a solenoid provided insignificant pull force. The pull force of the servo is more than enough to release the ram mass. The servo and servo control is situated near the axis of the centrifuge to limit the exposure to high g-levels.

Ram mass system

The ram mass system consists out of three main components; the ram mass, the ram mass guiding beam and the guiding beam fixation. The ram mass guiding beam is 10 mm diameter silver steel beam with a length of 210 mm. Silver steel was used as it produces less friction than normal steel. The ram mass guiding beam has 45 mm of M10 thread on one side to connect it to the guiding beam fixation. The ram mass guiding beam limits the horizontal movement of the ram mass ensuring that it only moves vertically. The guiding beam fixation is a circular plate that is bolted to the top plate of the centrifuge carriage. In the centre of the plate a M10 threaded hole is present for the fixation of the ram mass guiding beam. A lock nut is put on the ram mass guiding beam to put the thread under tension and prevent loosening due to vibrations. The guiding beam fixation plate has an additional function as it also accommodates the fixation of the pile displacement sensor.

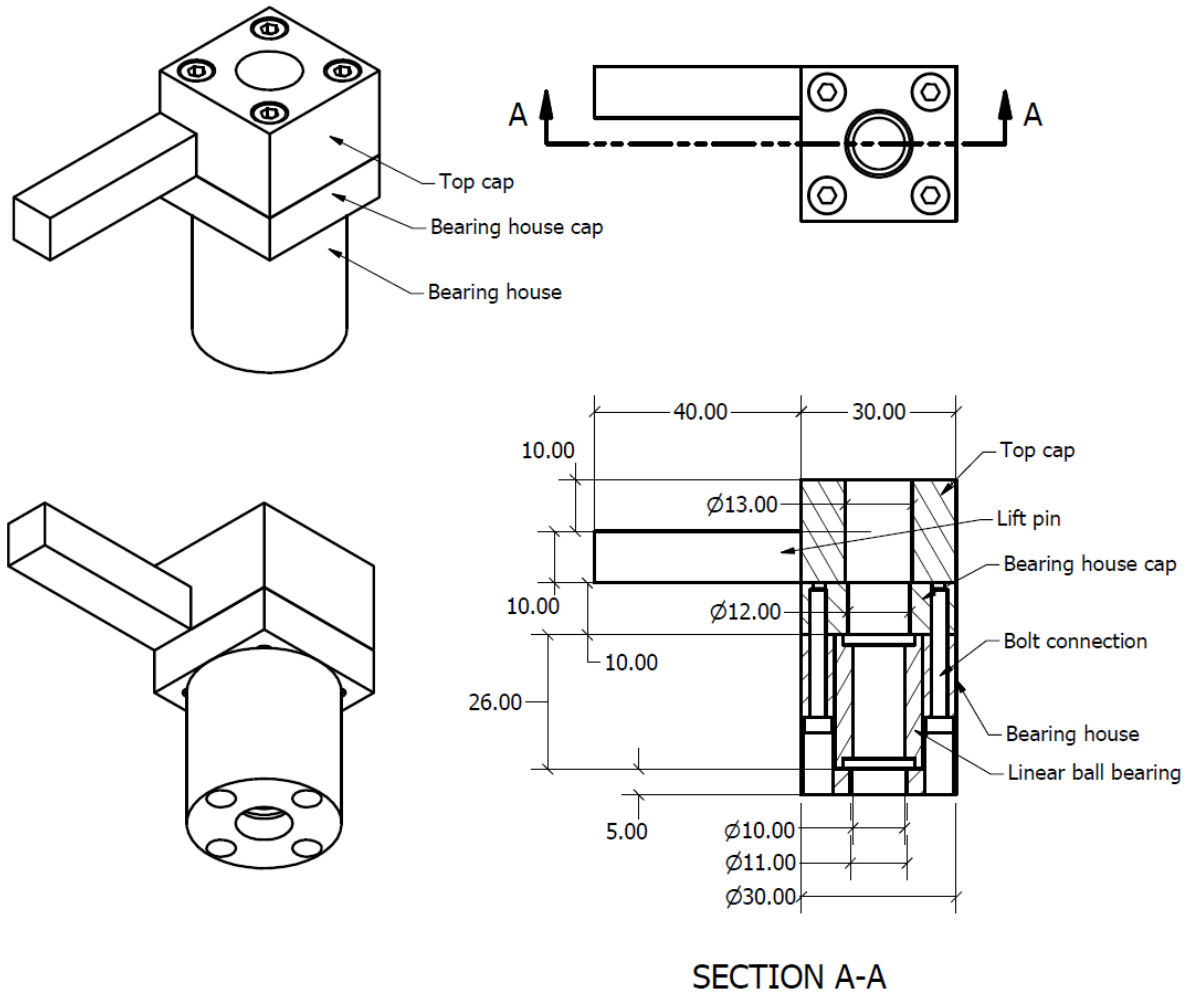

Figure 7 Detailed view Ram mass. Dimensions in mm

A modular system was created for the ram mass consisting of a bearing house, bearing house cap and a top cap. Figure 7 shows a section view of the ram mass. The bearing house contains a linear ball bearing by SKF to provide low friction interaction between the ram mass and the ram mass guiding beam. The linear ball bearing doesn't prevent rotational movement in the horizontal plane of the ram mass. To limit rotational movement a guide beam has been placed on the motor housing. Rotational movement would interfere with the function of the pile driving hammer. The bottom of the bearing house functions as the striking surface for the ram mass during driving. The bearing house cap fixates the linear ball bearing and provides the attachment of the top cap.

The total mass of the bearing house and bearing house cap is kept to a minimum of 60 grams by using aluminium. To achieve the desired mass a top cap is bolted to the bearing house cap. The top cap has the additional function of providing the pin that connects to the notch of the flywheel. Both the top cap and the bearing house cap are square while the bearing housing is circular. Three different top caps were made to allow a ram mass' mass of 110 gram, 140 gram or 220 grams. The top cap was manufactured out of steel. As it also has the function of lift pin and is put under quite high shock loads, the strength and stiffness of aluminium was not sufficient. By using steel the total volume of material needed to be added was also kept to a minimum. The modular system makes it possible to change the blow energy in between tests and also accommodate different masses for future research without the necessity of major alterations to the ram mass. The 110 grams is the minimum mass with the current design of the ram mass. This could be reduced further but would require a redesign of the ram mass.

Pile system

The pile-anvil system consists out of four main components; the pile, the pile cap, the motor-pile connection and the pile guide. The model pile has an outer and an inside diameter of 41.4 and 36.2 mm respectively, with a length of 190 mm. The pile can be imbedded up to 120 mm. Height restrictions within the carriage of the centrifuge prevented a longer pile. These dimensions were determined on the basis of the limitations due to particle size in section 3.1. A t/D_{50} = 24 and a D_o/D_{50} = 400 are achieved with these dimensions, satisfying the ratios stated before. The wall thickness of 2.5 mm gives D_o/t = 16.48. This is at the lower boundary of what is normal for open ended steel piles. While it might have been favourable to make the wall thickness less to stay closer to the ratios found in the field the current ratio is still within in the limits and ensures proper scaling of the soil behaviour. Secondly an initial plan was to embed sensors into the pile wall and that required a minimum thickness. These considerations are further explained in the following section on the instrumentation.

The pile is restricted from horizontal movement by the pile guide. The pile guide is a 79*30*350 mm^3 PVC beam with a hole in the centre. The hole is lined with a Teflon bearing ring. The pile guide sits on top of the sample container centering the pile in the soil sample.

On top of the pile sits the pile cap. Figure 8 show a section view of the pile cap. The pile cap slides into the pile and has a flange that rests on top of the pile. Above this flange the pile cap continuous to house several sensors. Finally a top plate closes off the anvil. The pile cap fulfils

several functions. Foremost the top plate of the anvil is the striking surface or anvil for the ram mass. Secondly it houses several sensors. The load cell that measures the blow force is situated between the top plate and the flange that rests on top of the pile.
On top of the top plate the impact speed sensor is situated. These sensors will be explained in detail in the next chapter. Lastly it functions as the connection point of the motor-pile connection. The motor-pile connection consists of a clamping ring and a rigid connection pin. The rigid connection pin is made out of M6 wire rod with the last 25 mm milled down to a 3 mm diameter. It is connected to the bottom of the motor housing. It slides into a 3.5 mm hole in the clamping ring. A 4 mm thick rubber ring on the 3 mm diameter end prevents steel on steel contact between the pin and the clamping ring. During pile driving the pin transfers the force resulting from lifting the ram mass into the pile through the clamping ring and the pile cap. It also maintains the correct height difference between the motor housing and the top plate of the anvil. The clamping ring sits between the top plate and the flange of the pile cap. Rubber between the ring and the pile cap ensures a tight connection between the two parts.

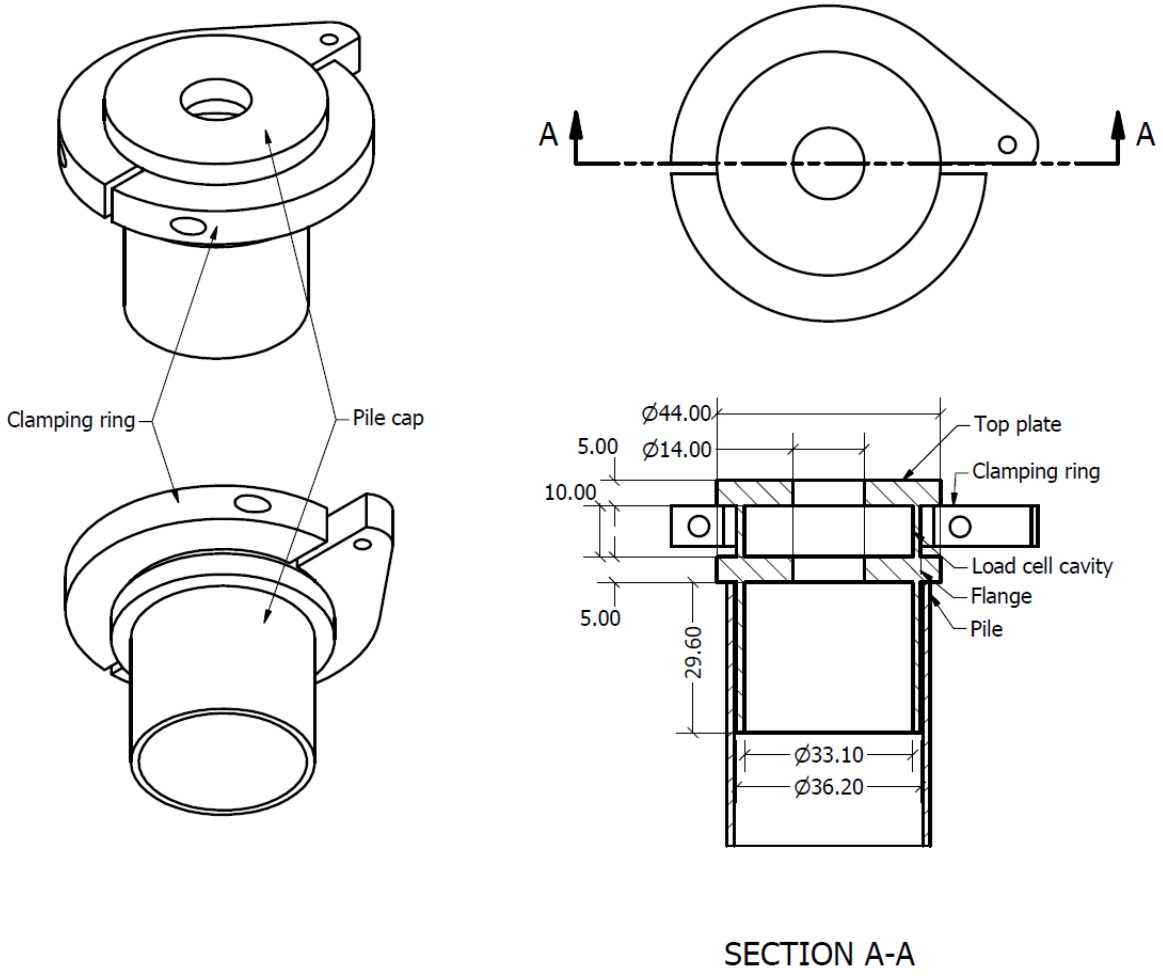

Figure 8 Detailed view pile cap and clamping ring. Dimensions in mm

Concept testing and modifications

As the whole pile driving hammer system was a new design and fabrication, extensive testing was done outside the centrifuge. In an initial system concept test, a secondary setup was used outside the centrifuge to better control and inspect the performance. The motor housing, ram mass and ram mass guiding beam were placed in a frame outside the centrifuge. Attached to the ram mass was a long spring that simulated the increased force and acceleration that would be present during centrifuge flight. During this test it became clear that the motor was incapable of repetitive lifting of the ram mass. Whilst the motor has the capability of delivering enough power to lift the ram mass at the relatively low 2100 RPM needed for 35 Hz blow rate, the motor controller does not.

As the power demand of the motor increases dramatically during lifting, more power is drawn from the battery which flows through the motor controller causing it to heat up significantly. A thermal fuse in place to prevent the motor controller from damaging is then activated stopping the motor. To prevent this from happening the motor needs to have a higher RPM so that the increase in power demand is less drastic. The electric motor is designed to deliver maximum power between 5000 and 8800 RPM. To achieve this a gearbox was installed in the motor housing. Instead of the direct coupling between the motor and the flywheel the power is now transferred through the gearbox. The gearbox has a ratio of 4.2 between in the incoming and outgoing shaft. Because of limited availability of gears the axle of the flywheel was increased on one end from 8 mm to 10 mm to be able to fit the gear properly. Furthermore an extra axle was placed in the motor housing to accommodate the gearbox. The gears on this axle were welded together so the power transfer was direct between the gears instead of going through the axle. This made the gearbox more robust as the gear axle connection proved a weak point. After the implementation the motor housing was again tested in the secondary setup. After minor adaptations of the gear axle connections on the flywheel, a constant blow rate was achieved. Because of the gearbox maximum blow rate has been decreased slightly to 30 Hz. This is due to the maximum RPM of the motor. It does provide a wider range of blow rates available. With the gearbox it is possible to achieve a blow rate between 10 and 30 Hz. This makes it possible to do a wider range of experiments.

After the 1g concept testing the entire setup was installed in the centrifuge and tested under higher gravity load. Several runs at different g-levels were done to check the installation of the setup and check all connections under the increased loading. An unexpected amount of friction was produced on the linear guide rail of the motor housing and the pulley that holds the counterweight cable. Because of this the motor housing didn't move down and followed the pile displacement as expected. To mitigate this the counterweight was reduced to 2.5 kg. After this several single blow tests were done to check free fall speed and workings of the ram mass release mechanism. These tests were successful and showed no major issues with the setup. Following this multiple blow tests were performed. Initial testing was done at 10 Hz blow rate. Both single blow and multiple blow tests were performed on a 90% relative density dry soil sample. As previously during 1g testing the pile driving hammer performed well during the multiple blow test. The downward motion of the motor housing was still not ideal but sufficient. A recommendation is proposed to mitigate this issue in chapter 5.

As the pile driving is a highly dynamic process with relatively high shock loads on many parts there is some wear on certain parts of the setup. The ram mass pin shows minor wear from repetitive contact with the notch. The notch itself show no wear from the contact. The wear of the ram mass doesn't significantly influence the workings of the setup. The ram mass guiding beam does show significant wear. Because the ram mass is lifted out of centre by the flywheel a moment is created that is exerted on the ram mass guiding beam. The hardened steel ball bearings are pushed into the softer silver steel of the guiding beam. This causes significant indentation on the guiding beam. The indentations influence the free fall of the ram mass. It lowers the impact speed of the ram mass up to 10% after several tests. It is still capable of achieving an impact speed high enough for the research purposes. During the performed tests this was mitigated by replacing the ram mass guiding beam after each test. An alternative to this is using a hardened steel guiding beam to prevent the wear. This does make it more difficult to machine and may negatively influence the life span of the ram mass linear bearing.

3.2.2 Instrumentation

For the test setup a new instrumentation system has been made. This not only involves the sensors but also the entire data acquisition system. The former setup installed in the centrifuge had a relatively low measurement frequency of 30 Hz. As the pile driving blow rate can be as high as 30 Hz it needed to be higher to accurately measure the different parameters. Especially the pile displacement, impact speed, impact load and pore pressure development needed a high measurement frequency. A measurement frequency of 10 kHz was determined as optimal. 10 kHz would give enough points to accurately measure the different aspects. A higher measurement rate would involve extensive alterations to the centrifuge system. Besides the fast measurement system the existing normal data acquisition measurement system still operates. In total 10 channels are available of which 4 capable of 10 kHz measurement rate and 6 of 30 Hz measurements.

Data acquisition system

The centrifuge system has two data acquisition systems, a “slow” and a “fast” system. The slow acquisition system has a scan rate of 10 kS/second meaning it scans the incoming channels 10,000 times per second. This is then internally averaged every 0.5 seconds. This decreases the size of the data making it possible to transmit directly to the centrifuge control computer over a wireless internet connection. The measurement resolution of this system is ca. 20 bits for the slow system. The slow system has 16 channels in total, 8 for high precision with a resolution of 18 bits or more and 8 channels with a lower resolution of 12 bits. The lower resolution channels are mainly used for less important tasks such as the RPM of the centrifuge.

The fast measurement system uses a four channel analogue to digital converter with a 12 bits resolution. The incoming signals are scaled per channel to maximize the measurement range. It has an internal memory of 8 Mbyte. Each data point requires 2 bytes of space. At a measurement frequency of 10kS/second 1 million data points can be saved. For the current setup this means a maximum of 100 seconds can be done. This is more than enough time for the driving of the pile to the desired depth. Because of the quantity of the data it is not possible to read it in real time. The data is transferred over the slip ring installation of the centrifuge. This is done at 720 scans per second which is ca. 14 times slower than the measurement speed. It can take considerable time to retrieve all the data and should be considered when making a test plan.

Sensors

The key parameters that needed to be measured during testing are the pore pressure development and the impulse given to pile by the ram mass. Pore pressure development can be measured using a pore pressure transducer and the impulse can be measured with a load cell above the pile. Besides these two main parameters several others are also of interest. Mainly the impact speed of the ram mass and the penetration of the pile. The impact speed of the ram mass can be used to determine the consistency of the hammer and back calculate the blow energy of the hammer. The displacement of the pile is of interest for similar reasons. It gives information about the amount and consistency of penetration. The combination of the data of the impulse, the impact speed and pile penetration gives a good overview of the behaviour of the pile and the hammer. As a final parameter the RPM of the motor is measured. This is of less interest to the

experimental results. It is mainly used to check the function of the hammer motor and to regulate the blow rate. The following section will discuss the design of these sensors in detail and discuss the measurement of the different parameters.

Pore pressure development

Pore pressure development is a vital parameter for this research. To measure pore pressure a pore pressure transducer (PPT) is used. PPT's have been used extensively in the past at the TUD centrifuge facility. For most research MPXH6250AC6T1 pressure sensor from NPX is used with a porous stone attached. The PPT combined with the porous stone is ca. 5*5*10 mm^3. The porous stone only allows pore fluid to enter the pressure chamber of the PPT thus giving the pore pressure. For positioning the PPTs two locations are possible. It can be either on the pile or in the soil. Both locations have their advantages and disadvantages.

When placing the PPT on the pile it can give a measurement straight along the pile and at a constant distance from the pile tip. This gives a good overview of the pore pressure during installation at several soil depths. However the PPT is relatively large compared to the pile. The PPT would need to be located in the inside of the pile and be in connection with the outside of the pile through an opening in the pile wall. The inside diameter of the pile is 36 mm. To fixate the PPT inside the pile it needs to imbedded in epoxy which would seal of most of the inside diameter of the pile. If not done this way the PPT would shear of during penetration of the pile. If more than one PPT would be installed this would mean almost completely closing of the inside of the pile. As it then would be a closed ended pile instead of an open ended pile this is not an option when using the conventional PPTs.

During this research contact was made with Harry Bos of Dike Monitoring and Conditioning systems (DMC). DMC uses fibre optic sensors to measure pore pressure development in dikes and embankments. This system is produced by FISO under the Evolution series. The Evolution system consists of a measurement module and separate fibre optic sensors. The measurement module provides the laser source for the sensor and reads the data from the fibre optic sensor. There are different fibre optic sensors for various measurements such as temperature, pressure and strain. The measurement is done at the end of the fibre optic cable. The fibre optic system is much smaller than conventional sensors with a diameter of only 1 mm. The small dimensions of the sensor makes it possible to implement it differently than conventional PPTs. Harry Bos was kind enough to provide us with two fibre optic pressure sensors and a measurement module for the use in this project. The provided measurement system has one limitation in that it has a low measurement frequency of 5 Hz. It is only viable to measure overall change in pore pressure development. FISO also produces a fast measurement frequency system but that was unfortunately outside the budget range for this project. To compensate PPTs would be placed in the soil to measure at a high frequency.

Because of the reduced size requirement of the fibre optic sensors new placement options are available. The wall thickness of the pile of the pile 2.5 mm. A 1.5 mm deep slit was machined into the wall of the pile. In this slit the fibre optic sensor was placed and fixated with adhesive. At the end of the slit a circular recess was made. On top of the recess 50 micrometres sieving mesh was placed. The mesh prevents any soil particles from interacting with the sensor. Only pore

fluid can exert pressure on the sensor. Two fibre optic sensor where placed in the pile wall using this method. One was placed at 1D, 41 mm, from the tip of the pile and one was placed at ca. 1.5D, 62 mm, from the pile tip.

Standard PPTs were used to provide fast measurement of the pore pressure development. Ideally the PPTs would need to be placed within less than 0.25D from the pile. As the PPTs are relatively large stiff elements in the soil model this would have adverse effect on the soil behaviour. To mitigate this an addition was made to the normal sensor layout. Instead of fixating the porous stone directly to PPT a hollow aluminium tube was placed in between. The aluminium tube has a length of 70 mm and a diameter of 4 mm. This makes it possible to place the relatively large PPT body outside the direct influence zone of the pile while still measuring the pore pressure close to the pile. Three PPTs were made using this configuration. The porous stone, aluminium tube and PPT pressure chamber were all filled with silicon oil using a vacuum chamber to ensure saturation and correct measurements. Figure 9 shows the PPT placed on struts for placement and the method used to place them in the sample.

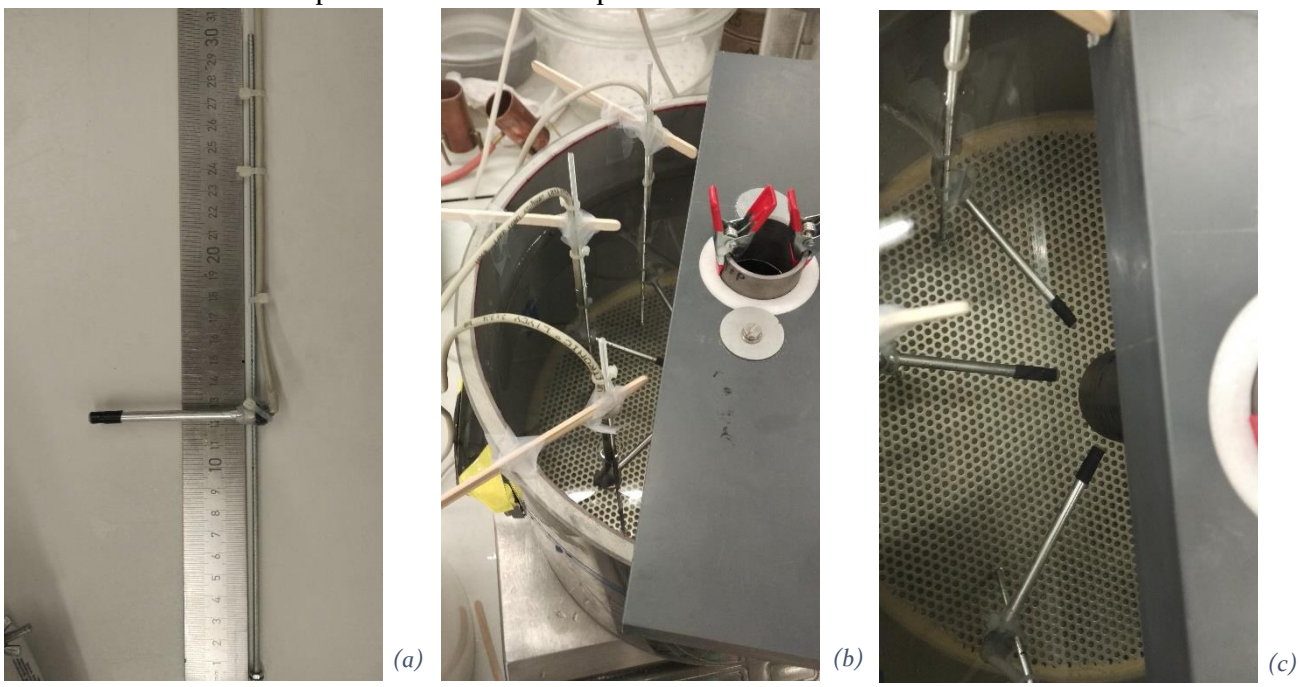

Figure 9 Pore Pressure Transducers. (a) shows the PPT placed on the strut with the elongation and porous stone at the end. (b) shows the placement of several PPTs in the sample container. (c) shows the vicinity to the pile possible with the PPTs. This is prior to the construction of the soil sample.

Unfortunately during system testing of the sensors the fibre optic sensors were pinched by the Teflon bearing ring that holds the pile. This broke the fibre optic cable. A full measurement during centrifuge testing has unfortunately not been made. During the duration of this project it was not possible to replace it. The fibre optic system should be investigated further as it shows great potential for further centrifuge research. All pore pressure measurements have been done with the adapted standard PPTs. Due to limited fast measurement channels only one PPT measures at 10 kHz. The other two PPT's measure at the low measurement frequency of 30 Hz.

Impact force

To compare the results of the experimental research and the numerical research it is important to measure the force going into the pile system from the ram mass. Three sensors are used to quantify this. First, a load cell is placed in the anvil of the pile system. Second, the impact speed of the ram mass is measured. Finally, the pile displacement is measured. This, combined with known parameters such as ram mass and blow rate, gives an accurate depiction of the force going into the system. Figure 10 shows the placement of the sensors.

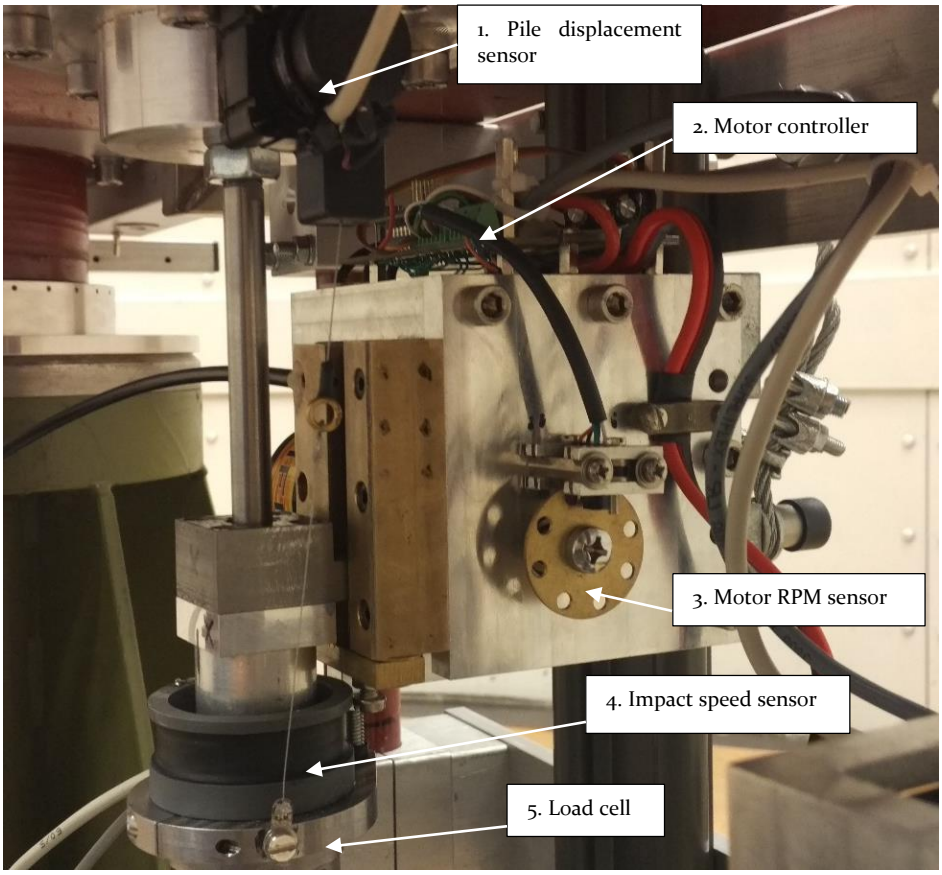

Figure 10 Overview Sensors

Load cell

The load cell in the anvil has been custom made for this project. It measures at 10 kHz measurement frequency. This is needed as the blow energy moves very quickly through the anvil. Even at this measurement frequency is still misses some peaks. Unfortunately limitations in the data acquisition system prevent a higher rate than 10 kHz. The load cell is made up of four Alteris FCB-2-11 strain gauges. These strain gauges incorporate two strain gauges in one holder making it possible to measure in two directions perpendicular to each other. In this setup strain can be measured both axially as radially. Both axial and radial strain gauges are configured in a separate full Wheatstone bridge. These bridges were then combined in another full Wheatstone bridge. This gives an average measurement of the entire load cell. An advantage of this setup is that it mitigates the effect of point contact between the anvil and the ram mass. Point contact gives compression and tension on different sides of the anvil which can happen relatively easily during driving. The load cell is directly incorporated in the anvil. The anvil consists of two pieces, a circular pipe with a flange and a top plate. The pipe ensures the position on the pile and the

flange provides the contact surface to transfer the blow energy into the pile. Above the flange the strain gauges are placed inside the pipe. The wall thickness of the pipe is 2 mm to ensure enough strain develops for the strain gauges. After placement of the strain gauges the top plate was placed on top of the pipe. Figure 11 shows the anvil before the top plate was placed showing the strain gauges. A special adhesive was used that has similar elastic properties to steel to prevent any changes in strain.

Figure 11 Open anvil with strain gauges inside.

Impact speed sensor

As the ram mass accelerates only under free fall it was important to have as little components interact with it. In the early design stage of the impact speed sensor a potentiometer was chosen to track the motion of the ram mass. This proved problematic as placement of the potentiometer on the setup was difficult and the interaction with the ram mass would interfere with the free fall. The potentiometer would also only give the location of the ram mass over time. Integration of this data would be needed to determine fall speed and acceleration. With the high blow frequency of 30 Hz this proved less than ideal. As the main parameter that needed to be measured was the speed at or just before impact with the anvil a new custom sensor was designed. Using the principle of an induction loop an impact speed sensor was designed. It consists of a PVC tube that sits on top of the anvil with a recess on the outside of the PVC tube. Within the recess 400 windings of 0.1 mm^2 copper wire are placed. This functions as a passive induction coil. At the bottom part of the bearing house of the ram mass four disc magnets with a height of 2 mm and a diameter of 5 mm were placed. The magnets were placed under a 90 degree angle of each other. As the ram mass passes through the passive coil it generates a current in the coil. This current can be measured at a high frequency and with a high resolution. Figure 12 shows the new sensor as well as its placement in the setup.

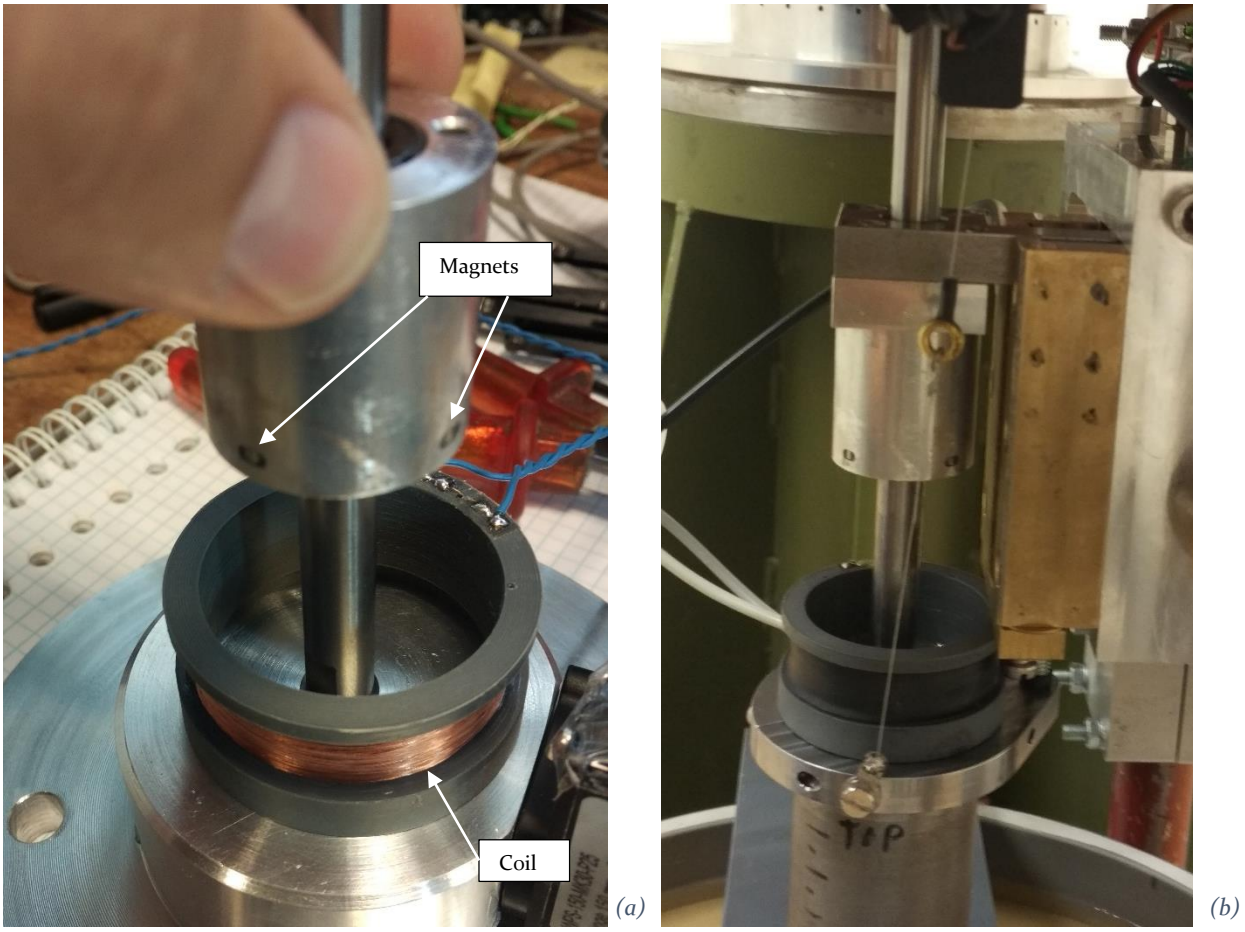

Figure 12 Impact speed sensor. (a) 400 windings of copper wire can be seen on the PVC housing. On the lower part of the ram mass magnets have been placed. (b) The final placement of the impact speed sensor on top of the pile cap.

For calibration purposes a secondary speed sensor was made. The second sensor used two light sensitive resistors (LDR) which were placed 10 mm apart behind a pinhole opening. This sensor was placed just above the induction coil. Calibration was done at 1g so the difference in location of the sensors would cause minimal problems. The ram mass was placed on a 1000 mm long silver steel guiding beam. At the bottom of the beam the anvil with the coil sensor and the LDR sensor was placed. An extra light source was placed to provide the LDR a constant bright light source. As the ram mass falls it first passes the LDR sensor. As it passes a change is seen in the LDR resistance. The difference in time when it passes the first and second LDR can be used to calculate the ram mass speed. Immediately after passing the LDR the ram mass passes through the induction coil. The ram mass was dropped from 5 different heights with 200 mm spacing. Each fall height was performed 5 to 10 times. Comparison between the calculated impact speed and the measurement from the LDR sensor showed that it accurately measured the impact speed. This was correlated to the signal from the induction coil. As the ram mass passes through the induction coil first a peak in voltage is measured after which a dale is measured. After several calibration tests it was found that the difference in voltage between the peak and the dale is constant for a certain passing speed. By placing the inductive coil 3 mm above the surface of the anvil it can give the speed of the ram mass just before impact. Because there is no physical impact with the ram mass the free fall acceleration is not influenced. In an earlier iteration of the sensor the LDR sensor was also a possibility to measure the impact speed. This was not chosen because

a constant light source is difficult to maintain during centrifuge operation. In addition, post processing of the data would have been troublesome.

Because of the principle behind the passive induction coil it is influenced by electromagnetic disturbances. During centrifuge operation is picks up the movement of the carriage through the earth magnetic field. There is also noise from the 1.2 kW electric motor that powers the hammer. This noise has an amplitude of ca. 0.01 V. The peak created by the ram mass is at least 0.2 V making the signal very clear in comparison to the noise. Moreover, the noise can be easily filtered out as the frequency and amplitude is known.

Pile displacement

The displacement of the pile after each blow is important to know. It gives input for comparison between the experimental model and pile driving models. Furthermore it is a safety aspect during the use of the experimental setup. The model pile has a maximum penetration of 150 mm before it hits the bottom of the sample container. Deeper penetration would damage the filtration layers at the bottom of the sample container.

Pile penetration is measured by a draw wire potentiometer. A WPS-150-MK30 by Micro-Epsilon was used. This sensor has a maximum measurement range of 150 mm. Penetration as measured relative to centrifuge carriage. The sensor is attached to the top plate of the carriage and connected with a high stiffness cable to the anvil. Special attention was given to the connections. A stiff hook and cable was used to limit extension in the system. The connection cable between the anvil and the sensor cable can be detached. This is needed to be able to place the sample container and the pile system. The potentiometer is spring loaded to retain tension on the cable. The upward force exerted by the spring and the added inertia of the sensor is insignificant in respect to the pile system.

Pile driving hammer instrumentation

The pile driving hammer is operated through the MP3 control program. To operate correctly during driving it is important to measure the revolutions per minute of the fly wheel. As the fly wheel picks up the ram mass it loses angular velocity and needs to provide additional power. The motor and controller already have a system in place to do something similar to do this but the frequency at which this is measured is to slow for the research purposes. To provide a direct response a RPM sensor has been attached to the fly wheel. The RPM measurement also helps keep the RPM constant during normal revolutions. As the motor rotates 4.2 times faster than the fly wheel because of the gear box an adjustment factor has been implemented.

The RPM sensor consists of a disc attached to the axle of the flywheel and a light sensitive sensor. In the disk eight openings are made with a 45 degree spacing. As the disc rotates the light sensor receives a signal each time an opening passes. This signal is converted to a RPM of the disc and thus of the fly wheel.

3.3 SAMPLE PREPARATION

For the development of pore pressures, it is important to have a fully saturated soil sample. Any air left in the system can greatly influence the development of pore pressure as air can be compressed so much more than water. When the pore fluid is water this can be relatively easily achieved by careful pluviation of the soil in water. After this the complete sample can be put under vacuum for several hours to extract any air left in the sample. In a centrifuge model water cannot be used as the pore fluid. In order to scale the pore pressure development correctly with the dynamic process of pile driving the permeability of the soil has been reduced. This can be done by either decreasing the permeability of the soil or by increasing the viscosity of the pore fluid. Decreasing the permeability of the soil can be difficult and possibly affects other soil parameters such as grain size, stiffness and strength. Therefore it is easier to change the viscosity of the pore fluid. Several possible pore fluids have been developed in the past to achieve this such as silicon oil.

For this research, the viscous fluid developed by Deltares (Allard & Schenkeveld , 1994) was used. The use of viscous fluid makes it harder to achieve a fully saturated sample using conventional methods. Using a dry pluviation directly in viscous fluid captures a large amount of air. Because of the small grain size of the sand it also floats on top of the fluid and doesn't settle evenly. When de-airing the sand-viscous fluid mixture large air bubbles move through the sample distorting the overall density. Previous research done at TU Delft centrifuge (Askarinejad et al, 2017) used a wet pluviation method where a deaired sand-viscous fluid mixture was pluviated submerged in a container filled with viscous fluid. Positive results were achieved with this method. However the size of the sample containers used for the current research needed to be at least thrice the volume than that of previous research. As sample preparation using the submerged pluviation method took 5-6 hours this was deemed too time intensive. An alternative to the submerged pluviation is the drizzle method developed by (Rietdijk et al, 2010). This method requires a special filtration layer at the bottom of the sample containers. As new containers needed to be constructed anyway to mitigate boundary conditions this filtration layer could easily be added to the design. The following subsection gives an overview of the sample preparation method and how it was implemented in the current research.

3.3.1 Method review

The method developed by (Rietdijk et al, 2010) consists out of three main steps. First a container is filled with a de-aired water-sand mixture. This mixture is pumped into a sample container filled with de-aired water using a peristaltic pump (Figure 13a). The sand settles evenly distributed in the container with relative density of 0%. The sample container has a filtration layer with an outlet at the bottom that lets water pass but not soil. As the water-sand mixture is pumped into the sample container the height of the water level in sample container is controlled by letting water flow through the outlet. Depending on the desired final relative density and height of the sample a certain amount of sand is pumped into the sample container. This is checked both by the height of the entire soil column and the increased weight of the sample container which is placed on a scale during the entire procedure. After this has been done the sample is densified. Because the pore fluid is still water this is relatively easy. Shockwave compaction is used to achieve the desired density. The sample container is lifted several centimetres and subsequently dropped. A shockwave then propagates through the soil sample

homogenously densifying it. This process is repeated until the desired density is reached. The density is checked by the height of the soil column. Excess pore fluid is drained through the outlet. This is one of the main benefits of this method as densification of a viscous saturated fluid is very difficult.

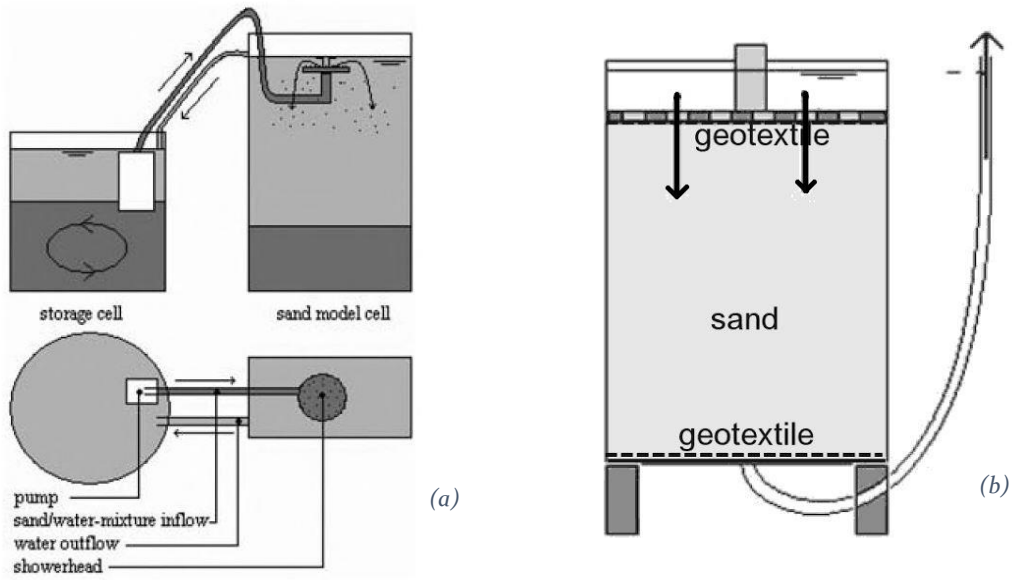

Figure 13 The drizzle method. (a) The water-sand mixture is pluviated in the sample container. (b) After shockwave compaction has been done, the water is displaced by viscous fluid from top to bottom. Adapted from Rietdijk et al. (2010)

The final step is to replace the water with viscous fluid (Figure 13b). First the water level is lowered until it at the soil level. A piece of geotextile is placed on the soil surface with a pump tube attached. Viscous fluid is pumped through the tube and the geotextile until a layer of ca. 10 mm is present on top of the soil. An additional pump tube has been connected to the outlet at the bottom in the meantime. As the surface layer of viscous fluid reaches the desired height water is extracted from the outlet into a water container. During this process the viscous fluid container, the sample container and the water container are all placed on scales. The scales indicate that the flow between the containers is equal. It is also used to check full saturation with viscous fluid. As the relative density of the sample is known the pore volume is also known. Pumping in the viscous fluid and extracting the water needs to be done at the same rate to ensure viscous saturation. This is done at a low pump rate. If the pumping rate is too high a drainage funnel can occur pulling through the viscous fluid without first displacing all the water. After having pumped through the total amount of pore volume pumping can be maintained to ensure that no water is left in the system. This can also be checked by taking a sample from the outlet tube. Viscous fluid feels different to the touch than water. During the pumping process this method can also be used to confirm no drainage funnel has occurred.

Three sample containers were made for this research. To mitigate boundary effects the containers were made as large as possible for the TUD centrifuge. Three circular containers with a diameter of 315 mm with a wall thickness of 10 mm and a bottom plate of 20 mm were constructed out of HDPE plastic. They have a free internal height of 175 mm. At the bottom of the sample container the filtration layer is installed to implement the drizzle method. The filter

layer consists of first a plastic grid that ensures a free space of 10 mm. This open space has a high hydraulic conductivity which enables an even flow from the top layers. On top of plastic grid 4 layers of mesh are present (Figure 14a). From bottom to top the mesh size is 3 mm, 150 micron, 50 micron and 3 mm. The 3 mm mesh is only used to fixate and protect the finer mesh from the sand. By going from a fine to a coarse mesh size it ensures that the filter doesn't get clogged with sand. A 15 mm recess was machined from the center to the edge of the bottom of the container and fitted with a 10 mm pipe. The pipe is fitted a valve at the end to connect a pump tube (Figure 14b). After the placement of the tube the recess was backfilled with a rigid composite to ensure structural integrity of the bottom plate.

Figure 14 Filtration layer. (a) Four layers of mesh to prevent the outflow of particles. (b) Outflow opening for extracting pore water from the bottom. A 10 mm plastic grid is placed on top of the bottom before placing the layers of mesh.

Independent of the relative density of the sample the height of the final soil sample is always 150 mm from the filtration layer. This is dictated by height restrictions within the centrifuge carriage. If it is saturated an additional 10 mm of viscous fluid is on top of the soil surface. Depending on the desired relative density the initial height before densification can be up to 181 mm. As this is higher than the internal height of the sample container an additional ring can placed on top of the container to increase the internal height to 210 mm. The total volume of each sample is 10.25 liter. Depending on the relative density the total weight of a saturated sample is between 19.1 and 20.8 kilograms. Using the sample preparation as described earlier it takes 3 to 4 hours to drizzle the sand in the sample container. The densification of the sample can be done within 15 minutes. Replacing the viscous fluid with water takes a relatively long time as pumping must be done at a low rate and with care. This takes at least three hours for a dense sample and as much as five hours for a loose sample. Because there is only a single outlet at the bottom of the sample container pump rate is lowered in steps during the process.

Any sensors that need to be embedded in the soil can be hanged in the container before the raining step. These will have limited effects on the quality of the sample. A disadvantage of the method is the high quantity of soil and viscous fluid that needs to be used as each preparation requires new sand, water and viscous fluid. Because of the small grain size and the nature of viscous fluid it is difficult and time consuming and to separate the two completely.

3.4 CONCLUSIONS

A new pile driving setup was successfully developed for the TU Delft centrifuge facility. It performs well and is able to model different prototype hammers and can be adapted to vary key pile driving characteristics. Blow rate, ram mass and blow energy can all be varied depending on the demands of the research. It can also be relatively easily adapted for future research where possibly different pile diameters or ram masses want to be used. There is wear on several parts but these components can easily be replaced with low cost. The main components of the setup are durable and can be used for many tests.

The instrumentation of the setup is capable of capturing key parameters in the pile driving process. Both the data acquisition system as well as the sensor system is capable of measuring at a desired acquisition rate. Proven sensors such as the pile displacement sensor as well as novel sensors such as the impact speed sensor work well in collaboration with the data acquisition system. A further optimization of the instrumentation could be found in the amount of “fast” channels and the time it takes to recover the data from the fast data acquisition system. This can take considerable time at the moment influencing the time between tests.

The drizzle method has been successfully adapted for use in the TU Delft centrifuge facility. Sample preparation using this method is relatively fast and efficient. It gives a good control over density and achieves a good saturation of the soil. Several samples can be prepared in series in a short time frame making it possible to perform a series of tests quickly.

4 EXPERIMENTAL RESULTS

This chapter presents the experimental results: subsection 4.1 gives an overview of the test that were done and details the sample properties; subsection 4.2 provides an overview of the several phases during multiple blow pile driving; subsection 4.3 presents the results from the pore pressure sensors; subsection 4.4 analyses the pile displacement; and, subsection 4.5 reviews the test program.

4.1 TEST OVERVIEW

Table 4 gives an overview of the tests that were done using the pile driving hammer. The ram mass number indicates which ram mass was used where 1 is the lightest 110 gram ram mass, 2 is 140 grams and 3 is the heaviest 220 gram ram mass.

Test Number	1	2	3	4	5	6	7	8	9	10
G level	20	50	30	50	50	50	50	50	50	50
Relative Density [%]	90	90	80	90	90	80-90	80-90	50-60	50-60	50-60
Pore fluid	None	None	None	Water	Water	Viscous	Viscous	Viscous	Viscous	Viscous
Ram mass	1	1	3	3	3	2	2	2	2	2
Blow rate [Hz]	10	10	Single blow	Single blow	Single blow	20	20	20	20	20

Table 4 Test overview

First, several concept tests were performed on dry sand. While the main focus of these tests was to check the performance of the pile driving hammer, the instrumentation system was in operation and soil parameters were controlled. The generated data can be used for this research. After concept testing, two tests were performed on dry sand. A single blow test was performed for validation of results of the work of (Azúa-Gonzalez, C. et al, 2017). Furthermore, two tests were done on a water saturated sample to check the PPT response and to see if there was any difference between dry and partially water saturated sand.

After these tests, five tests were performed on soil samples saturated with viscous fluid, test 6 to 10. Three tests, 8 to 10, were performed with PPTs in place to measure pore fluid pressure. These tests were all performed on the same soil sample. After several seconds of continuous pile driving the hammer and centrifuge were stopped and the setup was inspected. After inspection the centrifuge was started again and a new test was performed. These three tests put next to each other give insight to the pore pressure development at different depths. Three PPTs were installed, PPT1, PPT2 and PPT3 at respectively 80, 100 and 125 mm from the bottom of the sample container. PPT1, PPT2 and PPT3 were located respectively 14, 13 and 22 mm from the pile wall. PPT3 was originally located closer to the pile wall but shifted slightly during sample preparation.

4.2 Pore Fluid Pressure Development

During tests 8, 9 and 10 pore pressures were measured. The sample was saturated with a viscous fluid to properly scale the pore fluid pressure development. The pile was initially embedded 15 mm in the soil at 1g. After this the centrifuge was started and accelerated to 193 RPM to achieve 50g in the middle of the soil sample. After stabilization of the sensor parameters continuous pile driving was commenced at 20 Hz. After ca. 6 seconds of pile driving hammering was halted and the centrifuge was stopped. The setup was inspected shortly for any broken parts or mishaps. Testing was then continued by driving the already embedded pile deeper into the soil. A total of three tests was done using this procedure. Table 5 gives an overview of the tests. Figure 15 shows a cross sectional view of the sample container with the total displacement of each test to scale. The placement and distance of the PPTs is also indicated. Because of an interface malfunction the fast measurement data of test 9 was unfortunately not saved. All data for test 9 is from the slow measurement system.

Test number	8	9	10
g-level	50	50	50
Density	50-60	50-60	50-60
Pore fluid	Viscous	Viscous	Viscous
Ram mass	2	2	2
Blow rate [Hz]	20	20	20
Total number of blows	140	Ca. 100	111
Average impact speed [m/s]	5.12	-	5.10
Embedment depth [mm]	15	37.6	54.6
Total pile displacement [mm]	21.6	16	20.9

Table 5 Overview test 8, 9 and 10

During multiple blow testing the test period can be divided into several phases. Figure 16 and Figure 17 show these phases for test 8 and test 10. These are similar for all multiple blow tests. In the first phase the centrifuge is started and the entire setup is accelerated to 50 g. The pile lowers slightly, ca. 1 mm, under its own weight during this phase. After the pile displacement and pore pressure has equalized the hammer motor is activated and the flywheel achieves the desired RPM. At point 1 indicated in the figure the ram mass is released. The actual pile driving is commenced at this point. During test 8 and test 10 there was an issue with the motor housing moving down along with the pile. This meant that at a certain point the ram mass no longer makes perfect strikes on the anvil. This difference can be clearly seen when looking at pile displacement and pore pressure.

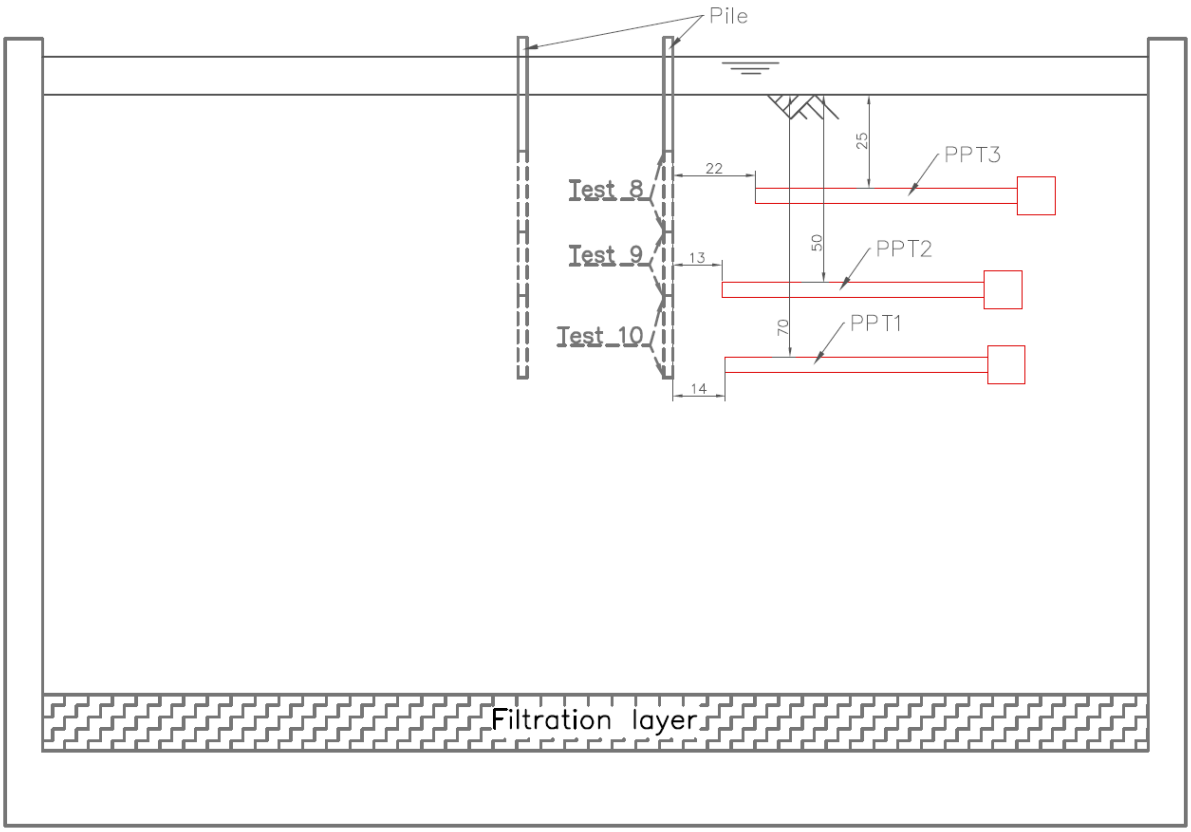

Figure 15 Overview test 8, 9 and 10. Cross sectional view of container with pile displacement during driving for all three tests with distances to PPTs indicated. Dimensions are at model scale.

The pore pressure displayed in these figures is from PPT1, the lowest PPT. Between point 1 and point 2 in Figure 16 and Figure 17 the ram mass is striking the anvil perfectly and transferring a large impulse to the pile system. There is a significant increase in pore pressure after each blow and also the pile displacement is consistent in both timing and quantity. At point 2 the distance between the motor housing and the anvil has become so large that the ram mass no longer makes full contact with the anvil. Energy is still transferred but at a lower level. There is still a gradual increase of pore pressure and the pile is moved but much less than before point 2. Because the ram mass is now not only striking the anvil but also the safety stop at the bottom of the guide rail on the motor housing energy is transferred into the motor housing. This energy is transferred partially through the motor-pile connection. The energy is enough to still increase the pore pressure but less than before. At point 4 pile driving stops completely. The motor is stopped and pile displacement maintains level. Pore pressure decreases gradually at this point. It dissipates until it reaches the value it had before driving commenced. This is not shown in the figures because the fast measurement stops before this point. This is visible in the slow measurement which measures from starting the centrifuge until it completely stops.

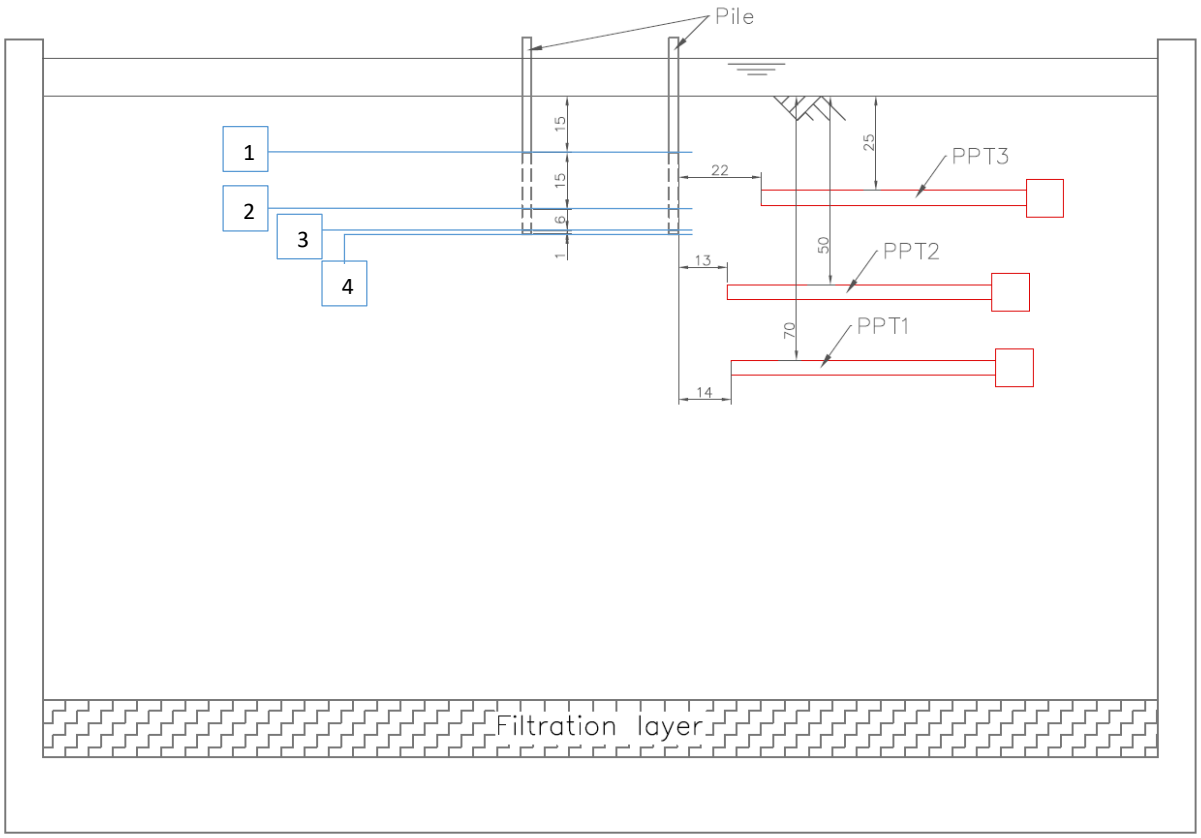

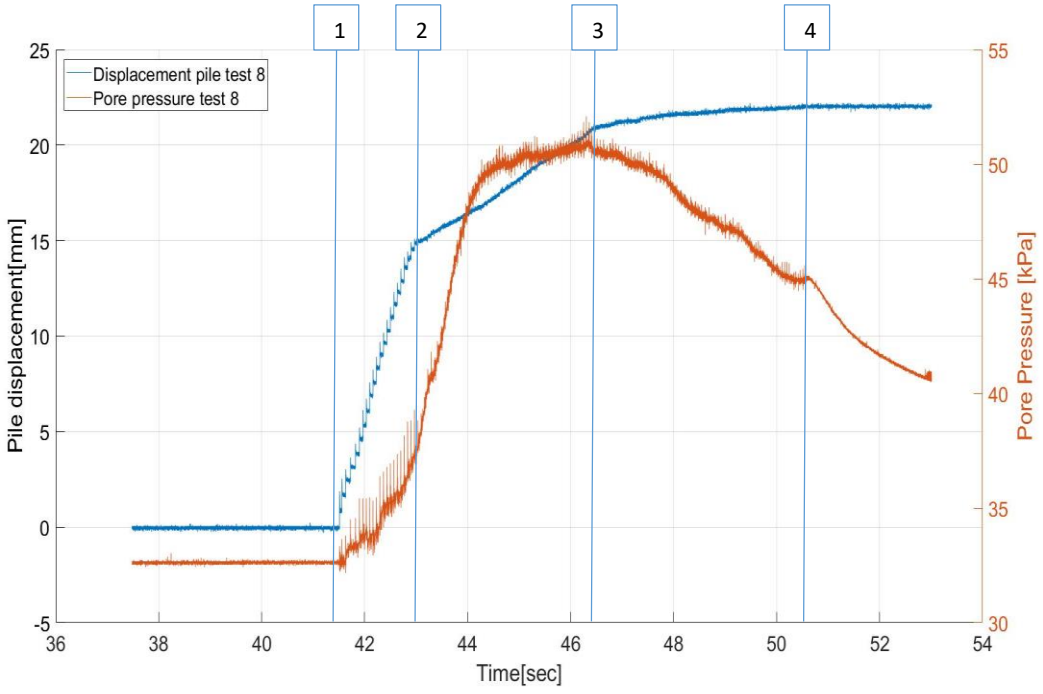

Figure 16 Test Phases Test 8. (a) Cross sectional view of container indicating the displacement of the pile during several phases of driving. (b) Pile displacement and pore pressure development at PPT1 during the different phases of driving. Dimensions are at model scale

(a)

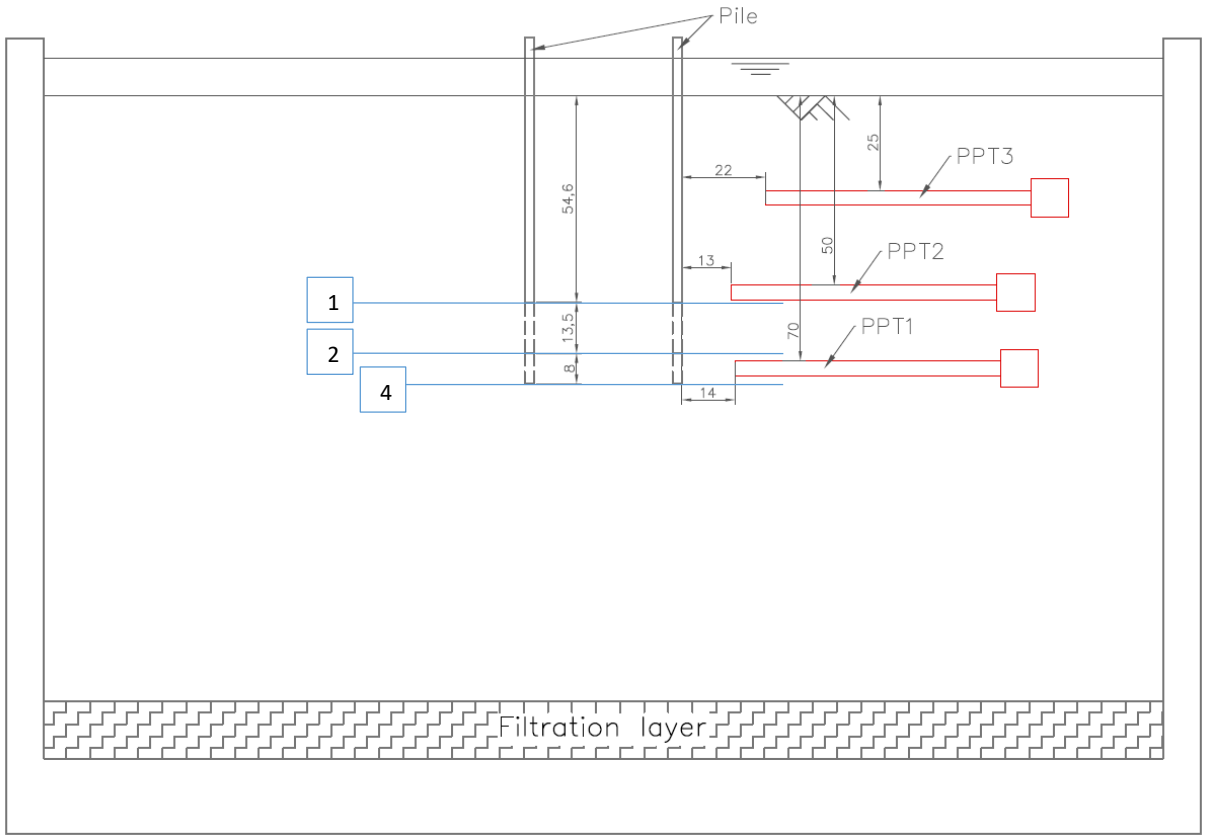

(b)

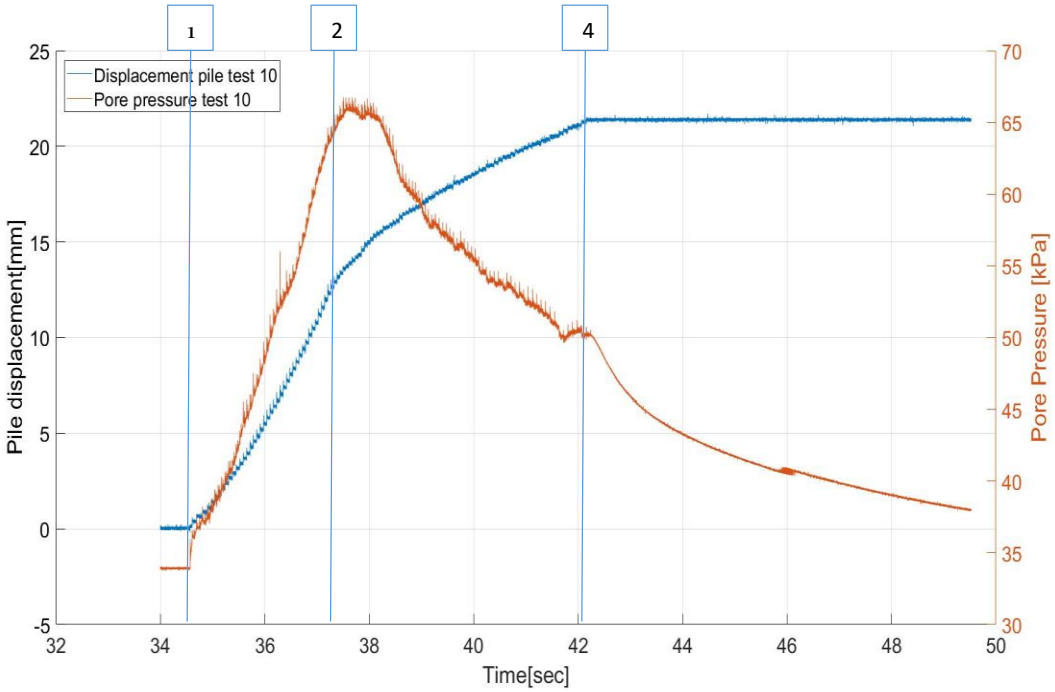

Figure 17 Test Phases Test 10 (a) cross sectional view of container indicating the displacement of the pile during several phases of driving. (b) Pile displacement and pore pressure development at PPT1 during the different phases of driving. Dimensions are at model scale.

Test 8 and test 10 differ in one aspect, test 8 has an additional phase at point 3. During test 10 the motor housing followed the pile system more closely while during test 8 the motor housing stayed at the same level. Energy was still transferred into the pile system through the motor-pile connection but not at significant level. After point 3 there is some pile displacement but not in the same quantity as before. Pore pressure continues to dissipate but with some noise from the energy transfer through the motor-pile connection. Pile driving was effectively stopped at point 3 during test 8.

The difference in the amount of energy transferred into the pile during the different stages of pile driving can make it difficult to compare the measurements. For that reason a first comparison is made only on the basis of the measurements done between point 1 and point 2 as indicated in Figure 16 and Figure 17. During these two points the energy transfer from the ram mass into the pile system can be stated as "ideal". Figure 18 shows the measurements from these time frames.

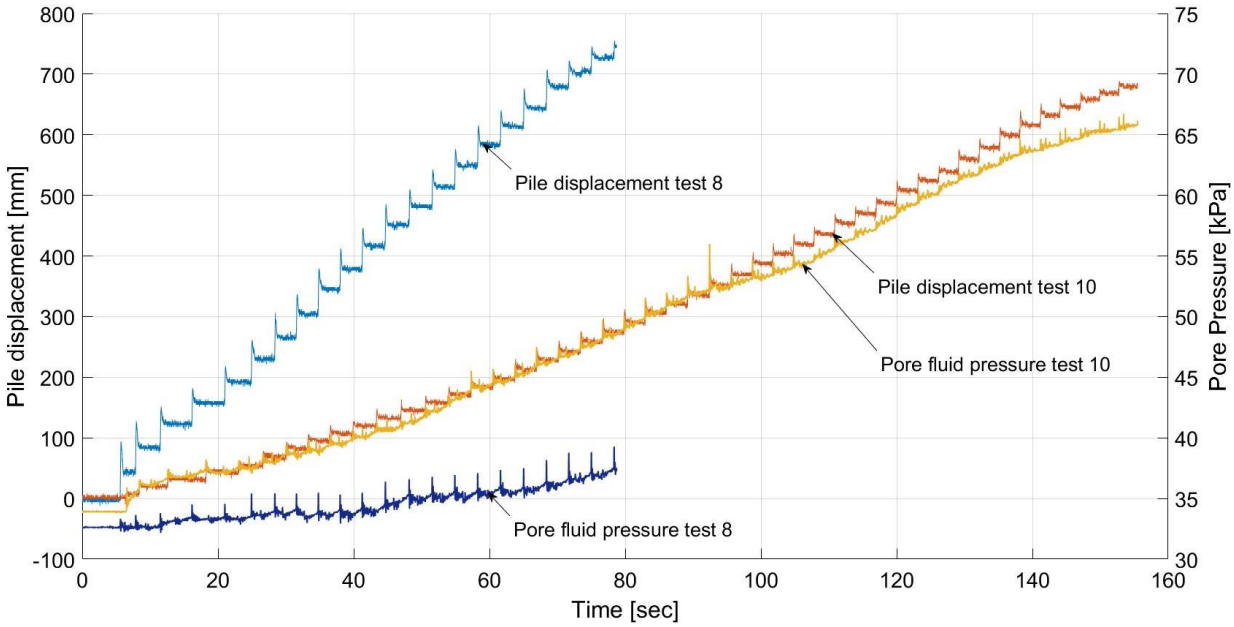

Figure 18 Pile displacement and pore pressure for test 8 and test 10 during ideal ram mass impact. PPT data is from PPT 1 measured at 10 kHz. Dimensions are at prototype scale.

From the figure several interesting phenomena can be identified. When looking at the pile displacement the difference in confining stress on the pile can clearly be seen. During test 8 the displacement for each blow is much larger than during test 10. The initial embedment for test 10 is much larger and thus the soil stresses working on the pile are much larger. This is both due to a larger surface of the pile is subjected to these stress and the force itself is larger. Because ideal pile driving is maintained longer during test 10 the final pile displacement is similar. It does however take ca. double the amount of blows. This effect was also seen in the pile displacement from test 6 and test 7. Secondly the influence of distance from the pile tip on pore fluid pressure can be seen. While the blow energy and blow rate are the same for both tests the development of PFP is much larger in test 10. The PPT data is from PPT 1 which during test 8 is at a much larger distance than during test 10. One of the main mechanisms behind the development of PFP is the shear stress exerted on the soil. This shear band around the pile is constrained in size and is thus also a more localized effect. While there is some development of PFP during test 8

this is probably mostly due wave propagation and less due to the shear stress exerted. In the time frame of test 10 the pile tip almost passes PPT1. Immediately from the first blow there is a sharp increase in PFP. This increase can be seen after each blow and keeps on developing during driving. Because of the vicinity of the sensor to the pile the effect of the shear stress is more profound and causes a large increase.

A correlation is present between the development of PFP and the distance from the observed point. This distance should be regarded in a radial distance meaning the shortest point to point distance from pile tip to sensor. Horizontal or vertical distance from the pile tip would misrepresent the actual distance from the pile tip. For a further comparison of this vicinity effect Figure 19 shows the slow measurement data of all the PPTs for all three tests. Because the slow measurement system does not have the required data acquisition frequency not each blow is captured. Furthermore it looks at the entire time frame of the test. Because of these aspects it should not be considered in a quantitated manner. However when looking at the measurement in a qualitative manner the vicinity trend found in the fast measurement data can be seen. Instead of looking at absolute pore fluid pressure the excess pore fluid pressure ratio R_u has been taken. R_u is a ratio between the change in PFP and the effective stress and gives an indication if liquefaction is achieved. When the ratio becomes 1 liquefaction occurs.

During test 8 where the pile is closest to PPT3 and also passes the PPT the largest increase in excess PFP ratio, EPFP, is seen. PPT1 and PPT 2 also react to the pile driving but less. Similar behaviour is observed during test 9 where the pile tip passes PPT 2. PPT3 measures less EPFP than during test 8 and PPT1 more. For test 10 PPT1 and PPT3 show similar behaviour as during test 8 and 9. As the distance to the pile tip decreases or increases, the EPFP respectively increases or decreases. For PPT2 this effect is seen less when comparing test 9 and test 10. Because the data is from the slow measurement system it is possible that a peak has been missed. The lack of difference could also be explained from the positioning of the PPT. PPT2 has the smallest horizontal distance from the pile wall at 13 mm. Furthermore is it closer to PPT 1 than PPT3. At the beginning of test 10 PPT2 is almost level with the pile tip. As driving commences the shear stresses are highest around the pile tip and could cause a large initial increases in EPFP. This initial increase can be seen in Figure 18 for example. The combination of this vicinity effect and the acquisition rate could explain the lack of difference in EPFP between test 9 and test 10 for PPT2.

.

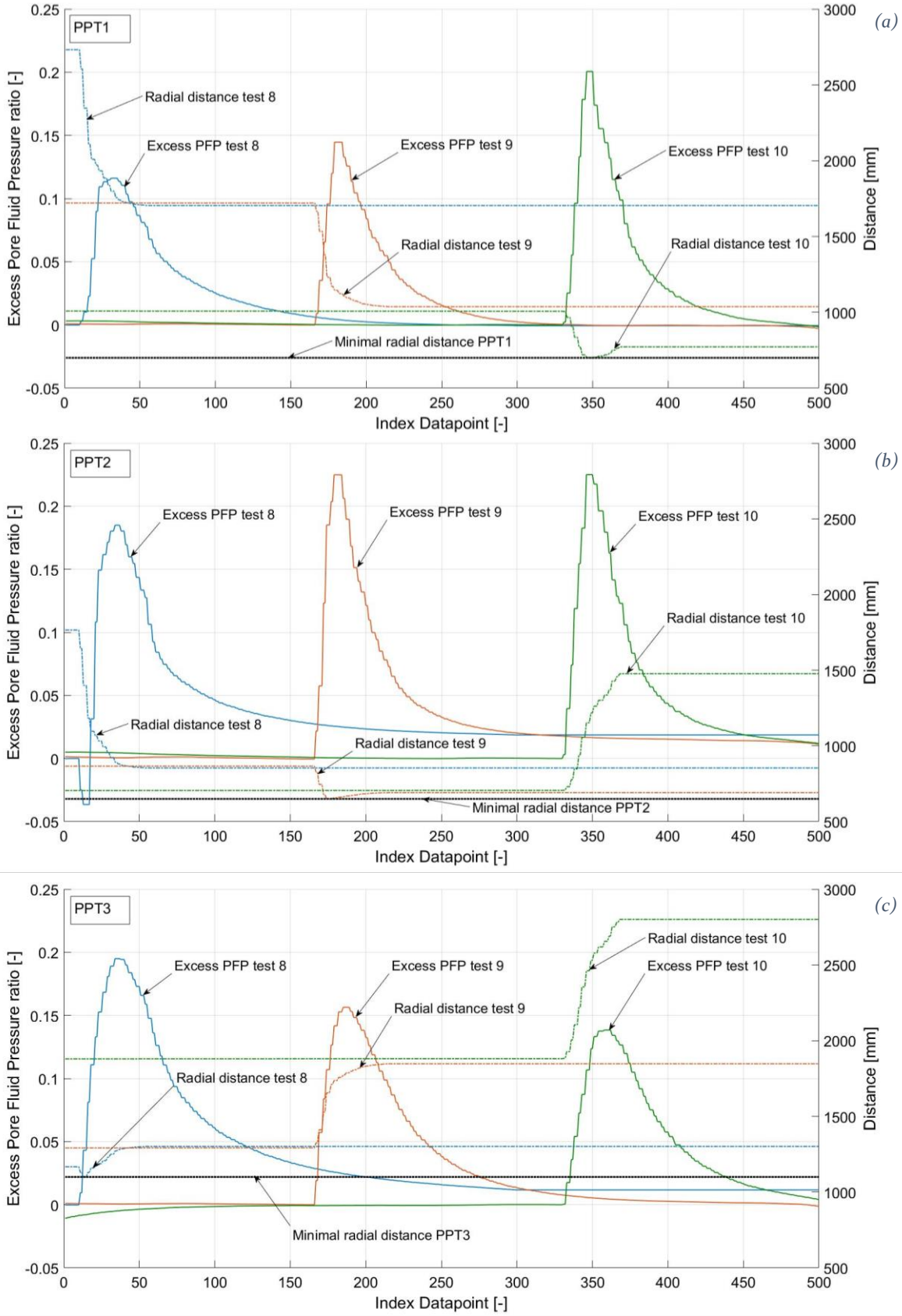

Figure 19 Excess PFP ratio and radial distance from pile tip to PPT. (a) shows the data for PPT1 from test 8, 9 & 10. (b) shows the data for PPT2 from test 8, 9 & 10. (c) shows the data for PPT3 from test 8, 9 & 10. Dimensions are in prototype scale.

The fast measurement system can give a more detailed view of the excess pore pressure development per blow. However only PPT1 was connected to the system limiting the possibility of comparing data. Also due to the loss of the data from test 9 the comparison is even more restricted. Figure 20 shows the fast measurement data from PPT1 from both test 8 and test 10. For the comparison with the slow data the entire time frame of pile driving is presented instead of the shortened time frame of Figure 18. The same trend that was visible from the slow measurement system is visible in the fast measurement data. The EPFP from this data is much higher than those in Figure 19. This makes apparent that the slow measurement system is not capable of catching the high peaks. The sample rate is not high enough. The effect of vicinity to the pile tip is again apparent when looking at the data. As the pile tip approaches the PPT, there is an increase in EPFP.

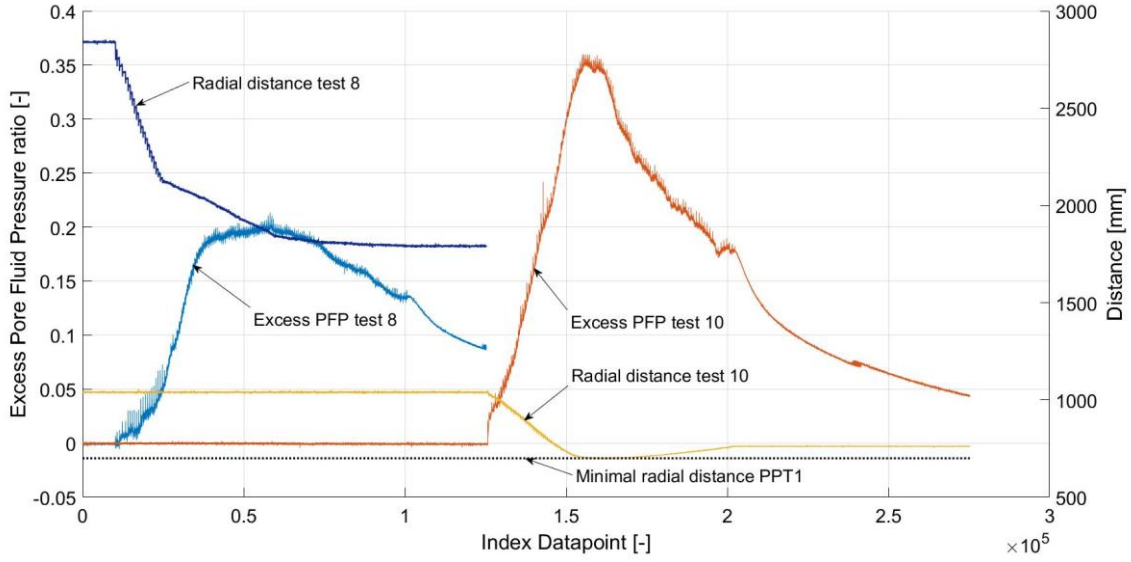

Figure 20 Detailed view Excess Pore Fluid Pressure development Test 8 and Test 10 for PPT1. Dimensions are at prototype scale.

This trend becomes even clearer when the EPFP is plotted against radial distance. When looking at the entire time frame of test 8 and test 10 an unfair comparison is made. In the different stages as mentioned before the energy transfer is not ideal. That is why Figure 21 only shows the EPFP between point 1 and point 2 where pile driving is ideal. Both the data from test 8 and test 10 is displayed. A trend can be seen indicated by the dashed line. Previous research on the relation between EPFP and radial distance from the source show a similar trend (Lamens, 2017). There is a slight delay until the data follows the trend line as the EPFP needs to build up. Furthermore there is ca. 0.1 second, model time, of data before pile driving commences included in the time frame.

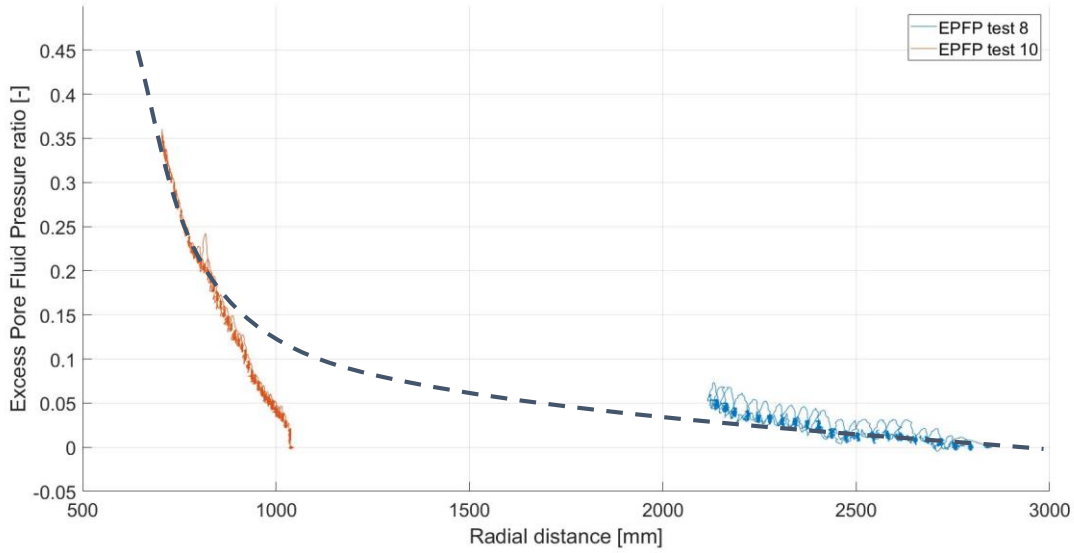

Figure 21 EPFP plotted against Radial distance. Data is constrained to the time between point 1 and point 2 where pile driving is ideal.

4.3 Pile Displacement

All tests measured pile displacement. This section will offer a short analysis of the resulting pile displacement data. Because tests were performed at different g-levels, all displacements are given at prototype scale in order to facilitate comparisons between results.

Figure 23 shows the single blow displacement of test 3 and test 5. These tests were done at respectively 30g and 50g. Furthermore, test 3 was done on a dry soil sample while test 5 was done on a water saturated sample. This makes direct comparison between these tests difficult. The difference in g level also influences the prototype scale. In test 3, the prototype pile is 1.2 m in diameter, while in test 5 the prototype pile is 2.1 m in diameter. Conversely, soil parameters are less influenced by the difference in g level. Soil behaviour is still within the scaling limitations of the setup. The peak displacement of the pile for test 3 and test 5 were respectively 40.4 and 198.5 mm. The main cause of this difference is not so much the difference in prototype scale but the difference in the ram mass speed. The setup is designed to achieve a maximum of 6.3 m/s impact speed at 50g. The mass of the ram mass is designed to deliver the correct amount of energy at this impact speed. At 30g the acceleration of the ram mass is of course much less. This results in a lower kinetic energy level at impact. During test 3 the ram mass had 47.460 Joule, prototype scale, of kinetic energy. During test 5 308.280 Joule of kinetic energy was achieved. This is more than 6 times the amount of energy that was transferred into the pile system. This explains the difference in pile displacement between these tests. The setup is capable of performing tests at a lower g level but other ram masses will be needed to compensate the loss of energy due to the decrease in impact speed.

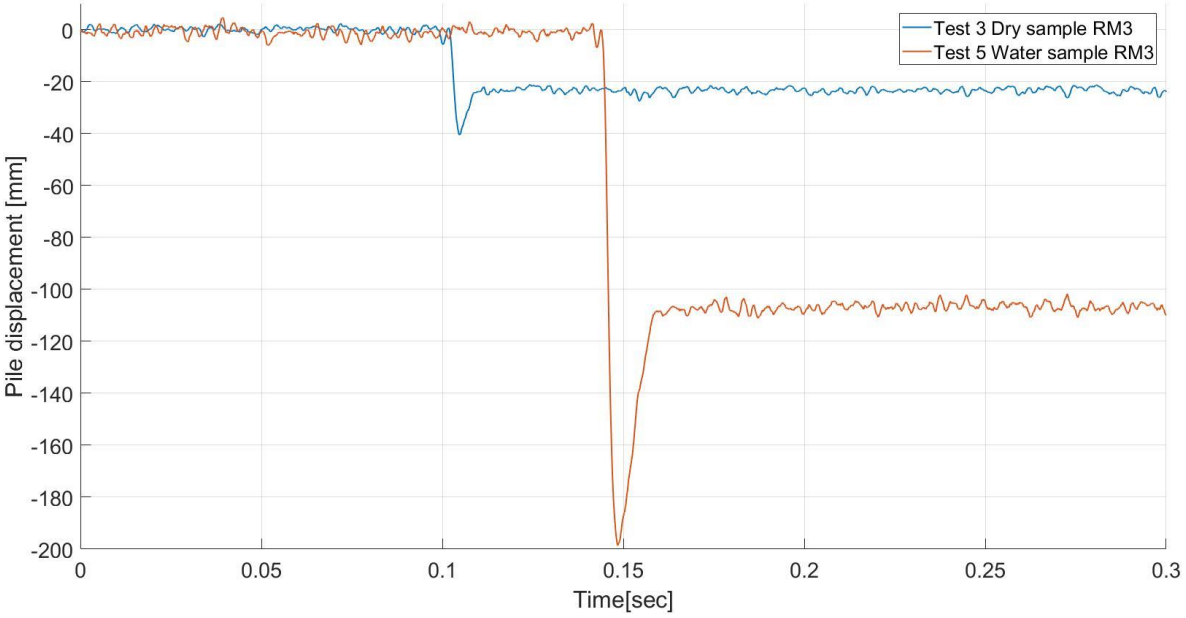

Figure 23 Pile Displacement Test 3 and test 5

A comparison has also been made with numerically modelled pile displacement with similar model parameters. (Azúa-Gonzalez C. , 2017) has performed Plaxis simulations based on the single blow tests. Comparison between the numerical simulations and the experimental model show a good correlation as can be seen in Figure 22. The pile displacement calculated and measured varied less than 10%.

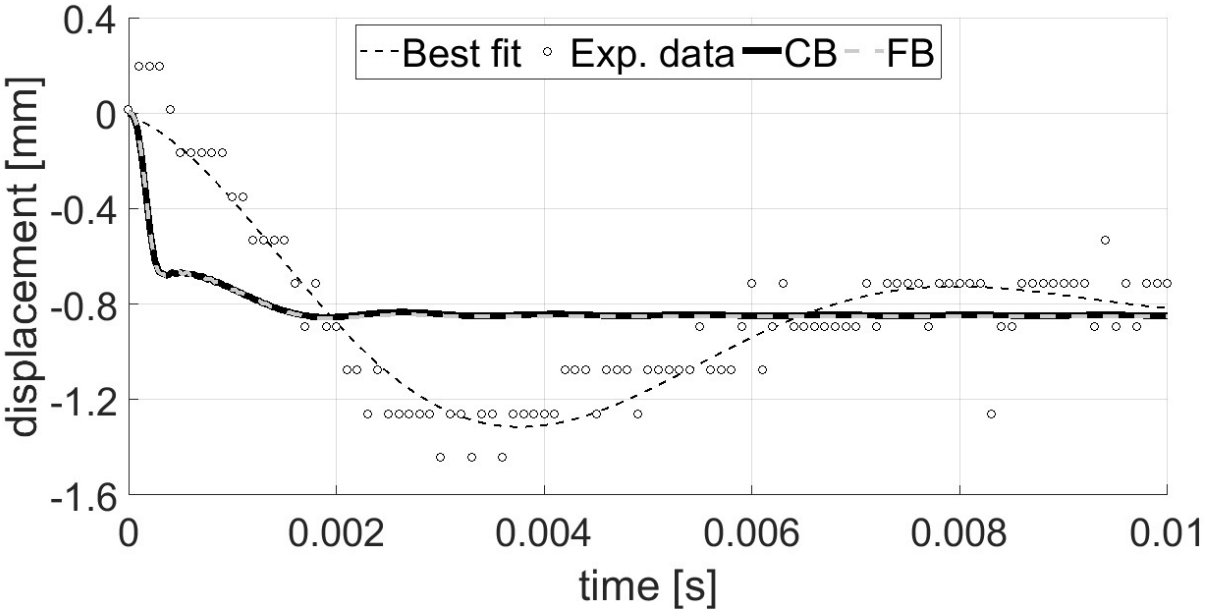

Figure 22 Comparison of numerical results and experimental data on pile head displacement on a single- blow centrifuge test. (Azúa-Gonzalez C. , 2017)

When looking at the multiple blow tests the increase of depth and thus soil stress becomes evident. Figure 25 shows the pile displacement during test 6 and 7. These tests were performed on the same sample after each other. Test 7 was performed on the already embedded pile of test 6 and thus at a deeper initial depth. The blow rate, ram mass and impact energy were similar during both tests. Both total displacement as well as the displacement per blow is much less during test 7 than during test 6. This can be seen very clearly during the first second of driving when the ram mass is still hitting the anvil fully.

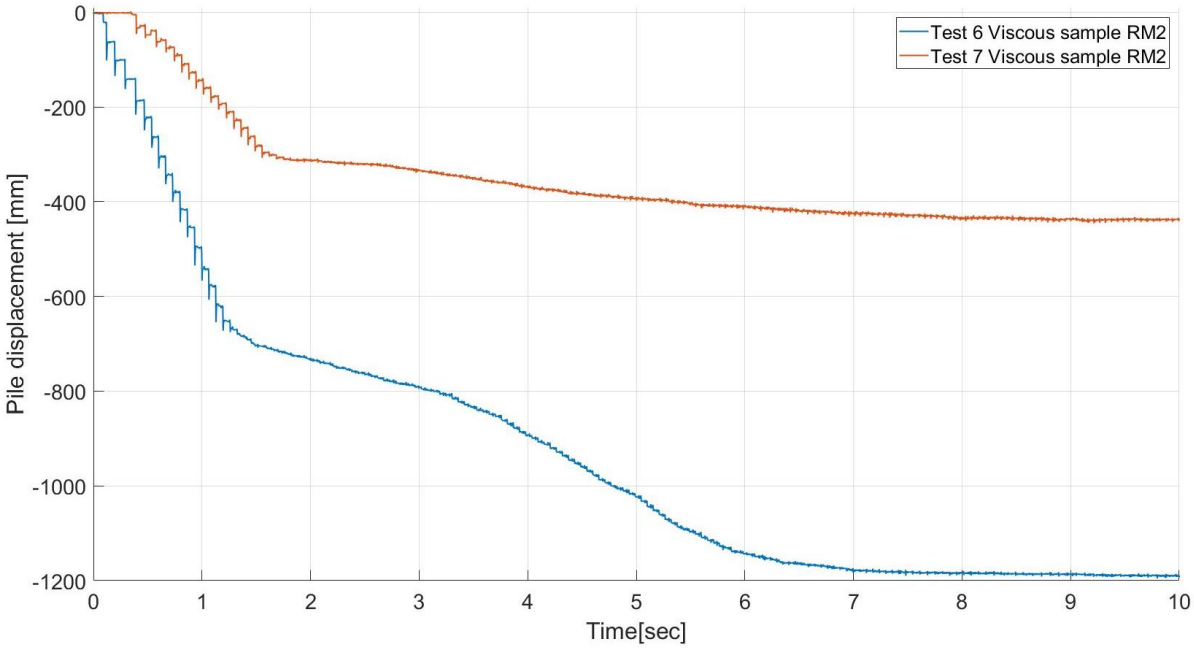

Figure 25 Pile Displacement Test 6 and test 7

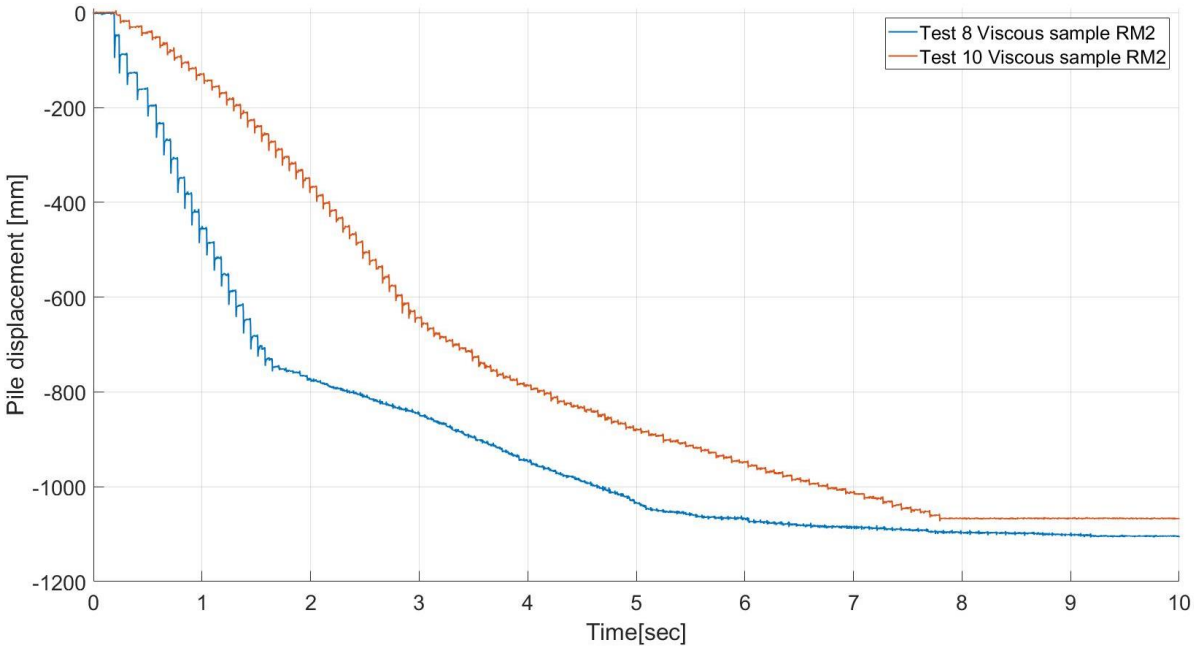

Figure 24 Pile Displacement Test 8 and test 10

This behaviour is also visible when comparing test 8 and test 10. Figure 24 shows the pile displacement during test 6 and 7. During the first 2 seconds of testing the ram mass is hitting the anvil fully. The displacement per blow is lower in test 10 than in test 8. The pile was initially embedded 750 mm in test 8 and 2730 mm in test 10. In total displacement test 10 does come closer than test 8. This is due to that the motor housing moved along with the pile and thus the ram mass and anvil make contact for a longer amount of time.

4.4 VALIDATION OF THE TEST SETUP

As the centrifuge model created during this thesis is new it still needs further validation. During the design of the model scaling laws and boundary conditions found in literature have been adhered to as closely as possible. However the current setup should be used to model an existing full scale case study. During normal installation of a full scale pile parameters such as blow rate and pile displacement are monitored. These can be used to check the validity of the model. A comparison of the pore fluid pressure is more difficult as this is normally not measured during installation. Because of the costs related to full scale testing this might prove more problematic. If a case study is found that can be modelled in the existing setup it would give valuable insight in the validity of the model.

Nevertheless the preliminary results presented do indicate that the setup can model impact pile driving correctly. Comparison made with the numerical study done by (Azúa-Gonzalez C. , 2017) shows high similarity. Furthermore pile displacement behaviour for various depths is as expected during driving. The magnitude of displacement is also in the correct scale for the prototype pile and hammer. From the measurements done during the performed tests, a clear connection can be found with the driving of a pile, the increase of PFP and the distance from the pile. These measurements fall within the range of expectations with what is found in literature. Based on these similarities it can be stated that the model behaves as expected and there is no major modelling error.

4.5 CONCLUSIONS

The setup has proven capable of driving a pile with a high degree of repeatability and consistency. Testing can be done with at several ram masses and at several blow rates. The minor problem with the movement of the motor housing – the motor housing does not move completely in sync with the pile – does not prevent successful testing. Single blow tests do not rely on the moving of the motor housing and for short multiple blow tests it is a manageable problem. Moreover, the motor housing problem is relatively easy to address, as is discussed in the recommendations on adaptations of the motor housing movement system below.

The instrumentation on the setup also performed well. Key parameters were captured with acceptable accuracy. The slow measurement system proved to be too slow to capture the higher frequency parameters, as was expected. The system nevertheless provides a good overview and is indispensable in monitoring the setup during testing. The fast measurement system was able to capture most data. It is desirable to add more channels to the fast measurement system to enable the capture of more PPT data at a high frequency measurement rate.

Further validation of the centrifuge model is needed. This could be done by modelling a case study. Preliminary results show no major modelling errors and soil behaviour is observed as expected. This indicates that the model is capable of correctly scaling the soil behaviour and pile behaviour of the prototype.

The tests that were performed were unfortunately not sufficient to conclusively describe the relationship between the development of pore pressure and the displacement per blow of the pile. The variation in parameters wasn't sufficient to quantify this relationship. While the displacement of the pile and the pressure wave resulting from driving is certainly the cause of the development of pore pressure, the influence of the excess pore pressure on the displacement of the pile is less clear. At a certain point, the excess pore pressure will influence the displacement but with the current set of tests it is not possible to determine which aspect of pile driving is the greatest contributing factor to the excess pore pressure. Further tests with a more varied parameter set, focused on varying the blow rate and ram mass, are needed to determine a correlation between the various pile driving characteristics and the development of excess pore pressures.

5 CONCLUSIONS AND RECOMMENDATIONS

This section presents conclusions and recommendations regarding experimental setup and the test results.

5.1 CONCLUSIONS AND RECOMMENDATIONS CENTRIFUGE SETUP

Several pile driving hammers have been developed at centrifuge facilities across the world. They vary wildly in blow rate, ram mass and blow energy. Blow rates vary from less than 1Hz to up to 30 Hz with ram masses varying from 70 grams up to 170 grams. These pile driving hammers can simulate small on shore hammers as well as larger off shore hammers. With the successful development of the new pile driving hammer for the TU Delft centrifuge an important addition has been made to the field: the hammer's combination of high blow rate and large ram mass is unique. The blow energy capacity of the hammer is large enough to model large off shore hammers but can also easily be changed to model smaller hammers. The blow rate can be accurately controlled making it possible to model soil behaviour such as pore pressure development. This makes it possible to use the setup for varying research purposes. The modularity of the hammer makes it possible to easily replace parts if they are broken but also redesign aspects to accommodate research needs that the current configuration cannot meet. This can all be done at minimum costs as the parts are small and easily fabricated. Even complete replacement of all the mechanical parts of the setup would not require a large financial budget.

The tandem development of both the instrumentation and the pile driving hammer means that these systems are deeply incorporated and work well together. Apart from using proven techniques to measure parameters such as the displacement sensor and the load cell also new techniques have been developed. A new type of impact speed sensor was designed and successfully implemented. This sensor makes it possible to measure the impact speed with minimal influence on the movement of the ram mass. Also the adaptation to existing pore pressure transducers has been proven effective. Pore pressures can be measured with a relatively cheap sensor close the pile without interfering the soil behaviour.

The experimental setup was successful on many levels. Nevertheless, two main improvements could be made.

First, control over the downward motion of the motor housing needs to be improved. As the motor housing only goes down due to its own resulting downward force, this process is not controlled and can cause issues during testing. It is difficult to correctly balance the motor housing, the counterweight and the spring. Also the motor housing makes it difficult to correctly place the spring in tests with piles embedded at a deeper level. To mitigate this issue, an extra servo could be placed that is connected to the cable connecting the motor housing and the counterweight. This servo would change the position of the motor housing. If the servo is coupled to the displacement sensor of the pile to receive the pile displacement it can reposition the motor housing. After each blow the displacement sensor would transmit the total displacement to the servo making it change the position of the motor housing. A concept design of the installation is presented in appendix D. By making this adaptation to the setup it would also mitigate the issues with the load cell. The extra force coming from the motor-pile

connection both because of the clamping connection as well as any force from the motor housing interfere decreases the quality of the load cell data. This can be resolved by implementing the proposed adaptation to the motor housing movement system which negates the need of the motor-pile connection. Because the motor housing is now controlled with the servo, the motor-pile connection is no longer needed. The clamping ring around the anvil could be removed and no force would be transferred through the connection into the anvil. A further design optimization of the load cell would likely also mitigate some of the noise aspects in the measurement. This would probably make the load cell measurement cleaner and more usable.

Second, the pile driving hammer has a maximum blow rate of 30 Hz. Whilst this was sufficient for the current research, it might be on the low side for future research. Changing this could be done by replacing the electric motor or by changing the gear ratio. Changing the gear ratio would be difficult as it would most probably require a different position of the gear axle. If this is needed a completely new motor housing has to be fabricated. There is an alternative motor made by Electrifly that might increase the RPM, the Rimfire 1.60. This version still fits within the motor housing and has the same bolt distances for attachment. It does require adjustments to the motor controller and a higher capacity battery to function. This would need to be tested. It may also be possible to achieve a slightly higher RPM by connecting a higher capacity battery to the current motor. The increased power could damage the motor and decrease its operational lifetime. But as the electric motor is relatively cheap it would be a minor risk.

5.2 Conclusions and Recommendations Test results

At an early stage of this research, ambitious goals were set. The initially planned test series encompassed more than 20 tests varying in soil density, blow rate and ram mass. In addition, a half pile setup was devised to examine the shear plane development along the pile during driving. These all were, and are, interesting research topics, which would have made it possible to draw more definitive conclusions on the influence of pore pressure development on pile driving. Unfortunately, the development of the setup required to perform these tests proved more time consuming and elaborate than initially thought. Going from a concept design to a fully working setup took the better part of 10 months, which reduced testing time.

The tests that were completed, combined with the numerical modelling by Carlos Azua Gonzalez, show that it is possible to perform accurate tests, which simulate the development of pore pressures as result of pile driving. Boundary conditions imposed by the sample container are limited and do not interfere significantly with the soil behaviour. The test series show that while further validation of the model is needed preliminary results show no major modelling errors. Installation parameters such as pile displacement and pore fluid pressure development are in the range as expected. Furthermore, a correlation was seen with the radial distance from the pile tip and the increase of pore pressure. This is a good starting point for future research.

Further tests with a varied parameter set are recommended. The variation that can be done is quite large as many aspects can be changed in regards to both the soil as well as the pile driving hammer. This parameter study could be undertaken through a PhD, or divided in smaller subsets that can be accomplished within a Bachelor or Master thesis. All experience and knowledge gained during this Master Thesis has been transcribed and can be properly

transferred to other researchers. As the basis of the setup is very simple, limited learning is needed in order to successfully test with it.

The following parameter studies should be undertaken:
First, the sample should be kept similar and only the blow rate should be varied. As the pore pressure dissipates over time it would be interesting to see how the variation of the most time dependent variable influences this. Based on these results it can be decided to first vary either the ram mass or the soil density. Varying the ram mass is relatively easy and additional ram masses can easily be made to further expand the parameter study. Varying the soil density will also have a large effect on the pore pressure development. The shearing mechanism partly responsible for the increase in pore pressure is highly dependable on the packing of the soil. The sample preparation method makes it possible to create homogenous samples with high accuracy and consistency. Performing tests with a loose, medium dense and dense sample would give a good insight on the soil behaviour.

After these tests series are concluded a further test series could be done with alternative piles. The setup can be adapted to fit smaller piles. In tandem with these studies the half pile setup could be fabricated. A new pile will need to be made for this research. The design of this pile can be found in the appendix and is a simple piece to fabricate. The analysis of the results using PIV would give valuable insight into the development of shear planes along the pile and the influence of boundary effects.

6 BIBLIOGRAPHY

Allard, M., & Schenkeveld , F. (1994). The Delft geotechnics model pore fluid for centrifuge tests. *Centrifuge*, 133-138.

Allersma, H. (1994). The university of Delft Geotechnical Centrifuge. *Centrifuge*, 47-52.

Askarinejad , A., Philia Boru Sitanggang, A., & Schenkeveld, F. (2017). Effect of pore fluid on the cyclic behaviour of laterally loaded offshore piles modelled in centrifuge. *19th International Conference on Soil Mechanics and Geotechnical Engineering*, (pp. 905-910). Seoul.

Askarinejad, A., Beck, A., & Springman, S. (2014). Scaling of static liquefaction mechanism in geocentrifuge and corresponding hydromechanical characterization of an unsaturated silty sand having a viscous pore fluid. *Canadian Geotechnical Journal*, 708-720.

Askarinejad, A., Laue, J., Zweidler, A., Iten, M., Bleiker, E., Buschor, H., & Springman, S. (2012). Physical modelling of rainfall induced landslides under controlled climatic conditions. *Eurofuge 2012.* Delft.

Attewel, P., & Farmer, I. (1973). Attenuation of ground vibrations from pile driving. *Ground Engineering*, 26-29.

Azúa-Gonzalez, C. (2017). *Dynamic finite element analysis of impact pile driving centrifuge tests.* TU Delft.

Azúa-Gonzalez, C., van Zeben, J., Alvarez Grima, M., Van 't Hof, C., & Askarinejad, A. (2017). Dynamic FE analysis of Soft Boundary Effects (SBE) on impact pile driving response in centrifuge tests. *9th Int. Conf. on Physical Modelling in Geotechnics.* London.

Bolton, M., & Lau, C. (1988). Scale effects arising from particle size. *Proceedings of the International Conference on Geotechnical Centrifuge Modelling.* Paris.

De Blaeij, T. (2013). *On the modelling of installation effects on laterally cyclic loaded monopoles.* Delft: TU Delft.

De Jager, R., Maghsoudloo, A., Askarinejad, A., & Molenkamp, F. (2017). Preliminary Results of Instrumented Laboratory Flow Slides. *Procedia Engineering*, (pp. 212-219).

De Nicola, A. (1996). *The performance of pipe piles in sand.* Australia: The University of Western Australia.

De Nicola, A., & Randolph, M. (1994). Development of a miniature pile driving actuator. *Centrifuge* (pp. 473-478). Rotterdam: Balkema.

De Nicola, A., & Randolph, M. (1997). The plugging behaviour. *Geotechnique*, (p. 841).

Dijkstra, J. (2009). *On the modelling of Pile Installation.* Technische Universiteit Delft.

Garnier, J., & König, D. (1998). Scale effects in piles and nails loading tests in sand. *Centrifuge 98*, -.

Garnier, J., Gaudin, c., Springman, S., Culligan, P., Goodings, D., Konig, D., Thorel, L. (2007). *Catalogue of scaling laws and similitude questions in geotechnical modelling* (Vols. IJPMG-International Journal of Physical Modelling in Geotechnics 3).

Haigh, S., & Madabhushi, S. (2002). Centrifuge modelling of lateral spreading past pile foundations. *International Conference on Physical Modelling in Geotechnics*.

Heerema, E. (1980). Predicting pile driveability: Heather as an illustration of friction fatigue. *Ground Engng 13*, (pp. 15-37).

Hwang, J., Liang, N., & Chen, C. (2001). *Ground response during pile driving* (Vol. Journal of Geotechnical and Geoenviromental Engineering).

Iskander, M. (2010). *Behaviour of Pipe Piles in sand.* Brooklyn: Springer.

Klinkvort, R., & Hededal, O. (2010). *Centrifuge modelling of offshore monopile foundation* (Vol. Frontiers in Offshore Geotechnics II.). Taylor and Francis.

Krapfenbauer, C. (2016). *Experimental Investigation of Static Liquefaction in Submarine Slopes.* ETH Zurich.

Kutter, B. (1992). Dynamic centrifuge modelling of geotechnical structures. *Transportation Research Record*.

Lamens, P. (2017). *Pile installation in submerged slopes,.* MSc. Thesis: TU Delft.

Levancher, D., Morice, Y., Favraud, C., & Thorel, L. (2008). A review of pile drivers for testing in centrifuge. *Xémes Journées Nationales Génie Cotier*, 573-583.

Maghsoudloo, A., Galavi, V., Hicks, M., & Askarinejad, A. (2017). Finite element simulation of static liquefaction of submerged sand slopes using a multilaminate model. *Proceedings of the 19th International Conference on Soil Mechanics and Geotechnical Engineering.* Seoul.

Moller, B., & Bergdahl, U. (1981). Dynamic Pore Pressures during pile driving in fine sand. *Proc. Int. Conf. on Soil mechanics and Foundation Engineering*, 791-794.

Muir Wood, D. (2004). *Geotechnical modelling, Volume 1.* Taylor and Francis.

Nguyen, C., van Lottum, H., van Tol, A., & Holscher, P. (2011). Centrifuge modelling of rapid load tests with piles in silt and sand. *Frontiers of Offshore Geotechnics II*, pp. 537-524.

Plantema, G. (1948). The occurence of Hydrodynamic Stresses in the Pore water of Sand Layer during Driving of Piles. *Proc. 2nd. Int Conf on Soil Mechanics and Foundation Engineering*, (pp. 127-128). Rotterdam.

Rietdijk, J., Schenkeveld, F., Schamineé, P., & Bezuijen, A. (2010). The drizzle method for sand preparation. *Physical modelling in Geotechnics*, 267-272.

Robinsky, E., & Morrison, C. (1964). Sand Displacement and Compaction around Model friction piles. *Canadian Geotechnical Journal*, 81-91.

Taylor, D. (1948). *Fundamentals of Soil Mechanics.* New York: John Wiley & Sons.

White, D. (2005). A general framework for shaft resistance on displacement piles in sand. *Proceeding of the 1st International Symposium on Frontiers in Offshore Geotechnics* (pp. 741-748). Taylor and Francis.

White, D., & Bolton, M. (2002). Observing friction fatigue on a jacked pile. *Centrifuge and Constitutive modelling: Two extremes* (pp. 347-354). Springman.

Wood, D. (2003). *Geotechnical modelling.* CRC Press.

7 APPENDICES

Appendix A Impact pile driving hammer manual
Appendix B Work drawings
Appendix C Concept design Motor housing movement system

Appendix A

Impact pile driving hammer manual

The following document details the function and test procedure of the impact pile driving hammer setup for the TU Delft centrifuge. It details the workings of the setup and the test protocol. For a detailed overview of the design please refer to the MSc. Thesis "Physical modelling of pore pressure development during impact pile driving using geo-centrifuge" by Joris van Zeben. For further information on the setup please contact Joris van Zeben by either email, jorisvanzeben@gmail.com, or telephone, 06 4277 1300. For technical support at the TU Delft contact Han de Visser, Kees van Beek or Ron van Leeuwen. Han de Visser has a general knowledge of the machine and the workings of the TU Delft geo centrifuge. Kees van Beek and Ron van Leeuwen have detailed knowledge of the workings of the setup and especially the electronics and sensor equipment.

Impact pile driving hammer setup

The pile driving setup consists out of three main elements: the pile driving hammer, the ram mass system, and the pile-anvil system. The pile driving hammer includes the motor housing, the load frame, ram mass release mechanism and the counterweight. The ram mass system includes the ram mass, the ram mass guiding beam and the guiding beam fixation. The pile system includes the pile, the pile cap, the motor-pile connection and the pile guide. A schematic overview is given in Figure 1. The entire setup and all needed bolts and other materials is in a labeled crate in the basement of the faculty of Civil Engineering. All materials needed are in labeled bags.

To install the setup in the centrifuge the following steps need to be taken.

- Attach the load frame with motor housing guide rail and pulley. Each clamp has four bolts that need to be tightened crosswise. The clamps consists of two aluminum parts that are not interchangeable. They are paired and numbered and should be used in that order. The bolts have rings and spring rings to assure proper connection. Check the presence of all these rings. Also check alignment of the motor housing guide rail with respect to the model pile. Also check if the rail is level both vertical and horizontal.
- Attach the counterweight bottom plate. Attach PVC tube to bottom plate. Make sure nothing falls in the tube as it is difficult to get out.
- Attach the ram mass guiding beam connection plate to the top plate of the centrifuge carriage. Make sure the potmeter is positioned correctly. It should point to the outside short side of the carriage.
- Slide the motor housing on the guide rail. A bolt can be slotted in the guide rail to keep the motor housing from going down.
- Attach the counterweight bolt to the motor housing. Make sure the bolt does not go in to far. If it protrudes too far on the insight it can hit the lift wheel.
- Attach counterweight and place inside the PVC tube.
- Attach the power and control cables to the motor controller. See Figure 3 for right order. Make sure all cables have enough slack as the entire motor housing will move a maximum of 12 cm vertical.
- Place the ram mass release mechanism near the center of the centrifuge. A position is already prepared on the aluminum shelf. Attach the control cables according to Figure 2. The ram mass release mechanism is powered by the battery pack. Keep this detached until actual testing commences. When placing the ram mass release mechanism take special

actual testing commences. When placing the ram mass release mechanism take special care of the placement of the black cable that is attached to the motor housing. This should have enough slack to let the carriage tip and the motor housing to move down. Furthermore it should not be able to hit the electric motor.

- Place the motor battery next to the ram mass release mechanism. Again take special care when attaching the motor power cable due to movement of the carriage and the motor housing. Do not connect the battery if not testing. Do not let exposed ends of the attached power line meet as this will give sparks and damage the battery.

The basis of the setup is now installed in the centrifuge. For the connection with the control mechanism of the centrifuge either Kees or Ron should be advised. For the placement of the pile and ram mass assembly please consult the test protocol. These need to be dismantled every time soil container is switched.

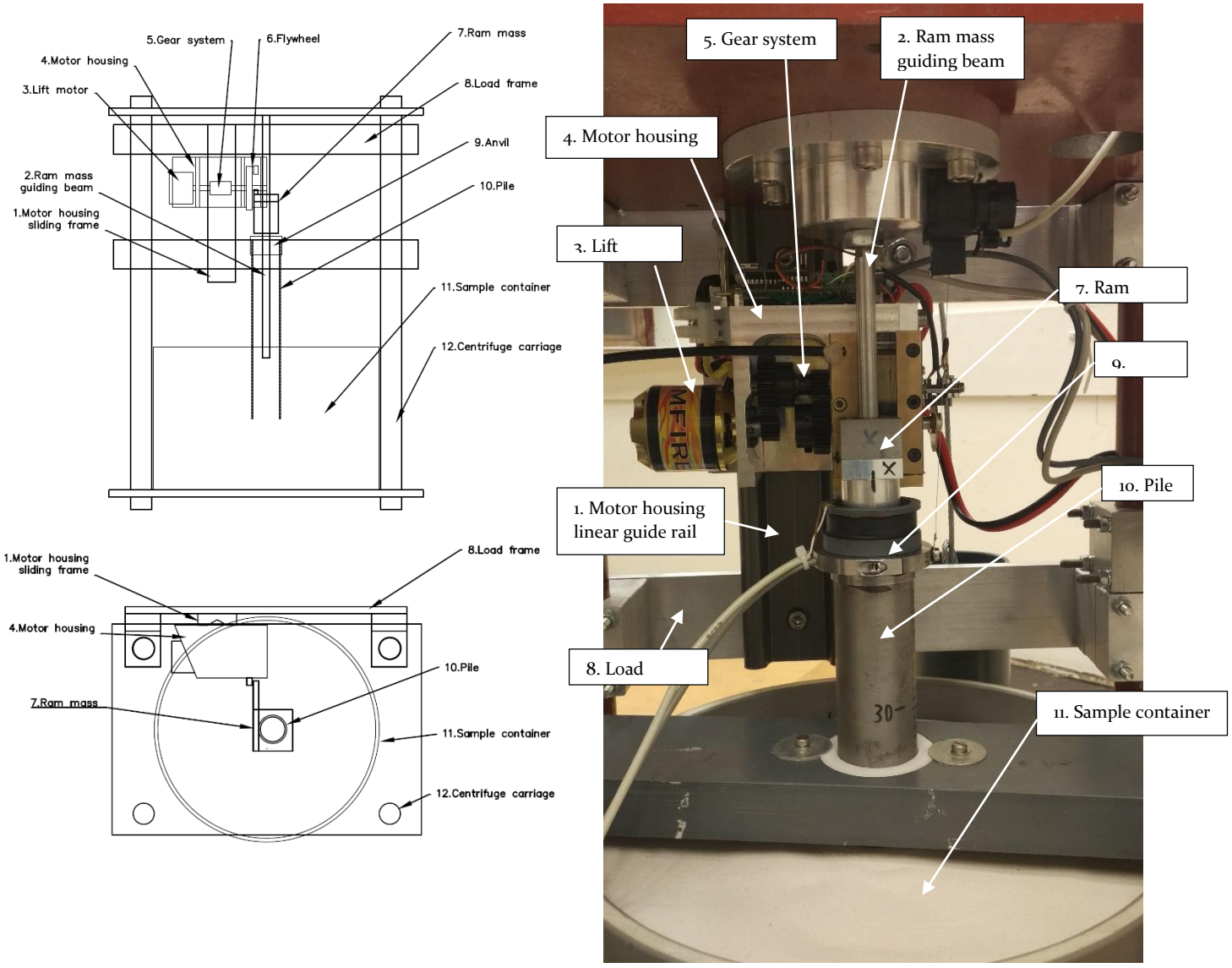

Figure 1 Schematic overview Impact pile driving hammer

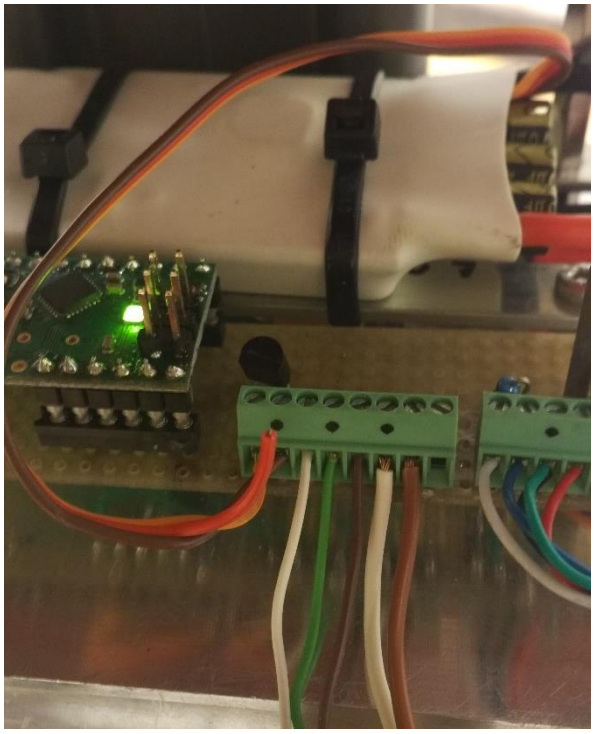

Figure 3 Cable positions on motor controller

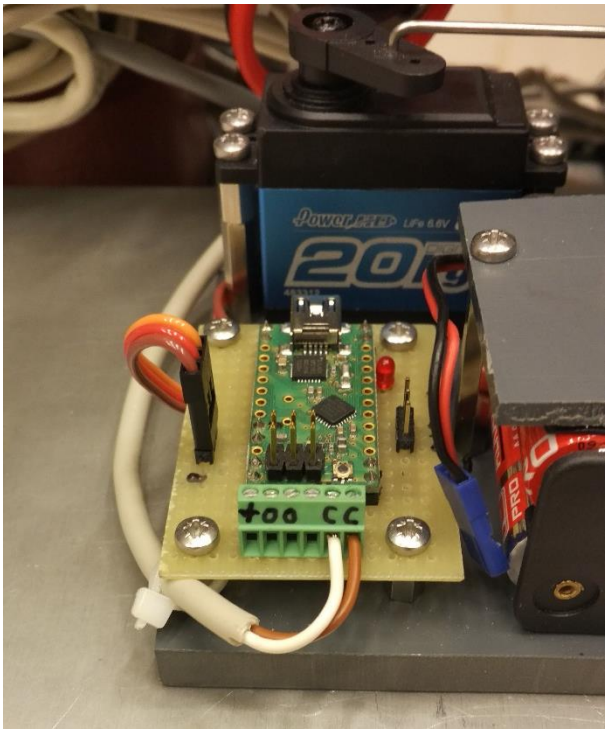

Figure 2 Cable positions on ram mass release mechanism

Several basic safety rules and operational aspects should be adhered when using the setup.

- **THE SETUP CAN NOT BE USED ABOVE 50g**. The entire setup is designed for 50g. Connections have been designed and tested for this g level. The hammer is also designed to work at this level. Going above this g level can cause serious damage.
- Check all bolt connections before each test. As it is a highly dynamic setup, bolts tend to shake loose. Especially the counterweight connections need to be checked regularly. If the counterweight comes loose it will cause serious damage to the centrifuge.
- The electronics on top of the motor housing are delicate. Take special care not to damage them.
- If you have any questions or doubts about the use or installation of the setup contact Joris van Zeben.
- The motor RPM is dependent on the charge of the battery. The battery does not deplete that quickly but should be charged regularly. A special charger is present.
- The setup has a considerable mass especially with the soil container. Always the counterweight in the other centrifuge carriage.
- The attached test protocol should be used as a checklist. For the safe and correct use of the setup it is important to check all the steps.
- The blow rate of the hammer can be changed by connecting a computer to the Motor controller. The correct USB cable is present in the storage box. Tera Term can be used to set the blow rate. Contact Kees van Beek to learn how to use Tera Term.

Test protocol Centrifuge pile driving hammer

Version 1.1, Joris van Zeben, 24-8-2017

Test Number:
Sample weight:
Ram mass number:
Centrifuge RPM/g level:
Blow Rate (Hz/RPM):
Type of sample (RD,Wet, viscous etc.):
Other remarks:

Preparation in the centrifuge

- □ Unscrew the central guiding beam from carriage
- □ Unscrew Motor pile connection
- □ Assemble pile guidance-pile-anvil-ram mass-guiding beam-guide beam nut system
- □ Place sample container
- □ Place pile system in sample container. Make sure ram mass is inserted into motor housing
- □ Attach central guiding beam onto carriage mounting
- □ Reattach motor pile connection.
- □ Attach draw wire sensor to anvil
- □ If present attach PPT's to sensor box and tie down with tie wraps
- □ Check all bolt connections especially
    - Central guiding beam bolt (1)
    - Ram mass bolts (2-4)
    - Motor pile connection bolts (2)
    - Counterweight bolt (1)
    - Counter spring bolts and nuts (2 bolts 4 nuts)
- □ Check position of motor block. Rubber of motor pile connection should be resting on the anvil
- □ Check free length of cables for motor block and anvil sensors
- □ For wet sample double check bottom plug is properly in
- □ Check balance weight in other centrifuge carriage
- □ Place ram mass in top position. Disconnecting the servo lets it move freely. Make sure the Release off command has been given in the control room before doing this
- □ For single blow action, check position of flywheel so that the ram mass can fall freely
- □ Attach power to servo and motor battery
- □ Switch on the GoPro and check position of both cameras
- □ Check the centrifuge chamber for all loose materials
- □ Check tool box for all tools and close the boxes.
- □ Start up centrifuge.
- □ Check if everything is alright in the centrifuge
- □ Leave the room and lock the door

Start-up procedure in control room

- □ Start up cameras
    - Camera in centrifuge room
    - Camera outside centrifuge room

    - Camera on centrifuge frame
- □ Launch Tera Term and check if data is coming in
- □ Zero all measurement channels in MP3
- □ Start new datafile and use the following coding
    - g level_SB/MB_RM%_VS/WS/DS_filenumber_Date
        - SB = single blow
        - MB = multiple blow
        - RM = ram mass(1 is lightest 3 is heaviest)
        - VS/WS/DS = Viscous sample water sample or dry sample
        - Date by yearmonthday
    - Eg. 50g_MB_RM3_WS_041
- □ Spin up centrifuge to desired g-level. This should be determined at half of pile embedment depth.
- □ Check on camera position of motor block. It may not have risen more than 5 mm(ca. thickness or rubber)
- □ Check if pile, motor and measurements are stable when desired g-level is reached
- □ Open Tera Term and prepare measurement. Commands are as following.
    - 1 = start recording
    - 2 = stop recording/playback
    - 3 = playback last measurement
- □ For multiple blow test activate motor with **Motor on** in MP3
- □ Check if the all measurement all still in order. With focus on the following;
    - Motor RPM
    - Centrifuge RPM
    - Pile displacement
    - Camera feed
- □ Press **1** in Tera Term and immediately afterwards press **Release On** in MP3
- □ Check pile displacement in MP3 and visual inspect motor and pile movement in camera image
- □ Press **Motor off** in MP3 if desired installation depth is achieved
- □ As quickly as possible press **2** in Tera Term. Write down the number of measurements
- □ Check if motor has stopped correctly through motor RPM measurement and visual inspection from the camera
- □ If test is concluded set centrifuge speed to zero and start slowing down the centrifuge
- □ In Tera Term press **File > Log** and use the same coding as before and add .csv at the end to start logging. When log is running press **3** to playback the last measurement log. This can take considerable time if file is large
- □ Check if centrifuge has slowed down. Press **Release off** in MP3
- □ Go down stairs to completely stop centrifuge
- □ Stop Go Pro
- □ Check the setup if everything is still were it is expected
- □ Prepare setup for next test

At the end of testing export files from MP3.
MP3 > Tools > Export data. Choose csv for output data. This is faster than choosing excel.

Appendix B

Work drawings

The following document gives an overview of the impact pile driving setup with detailed work drawings. Digital copies of these drawings and a full 3D model are available at TU Delft and IHC MTI. For more information please contact Joris van Zeben, jorisvanzeben@gmail.com, 0642771300.

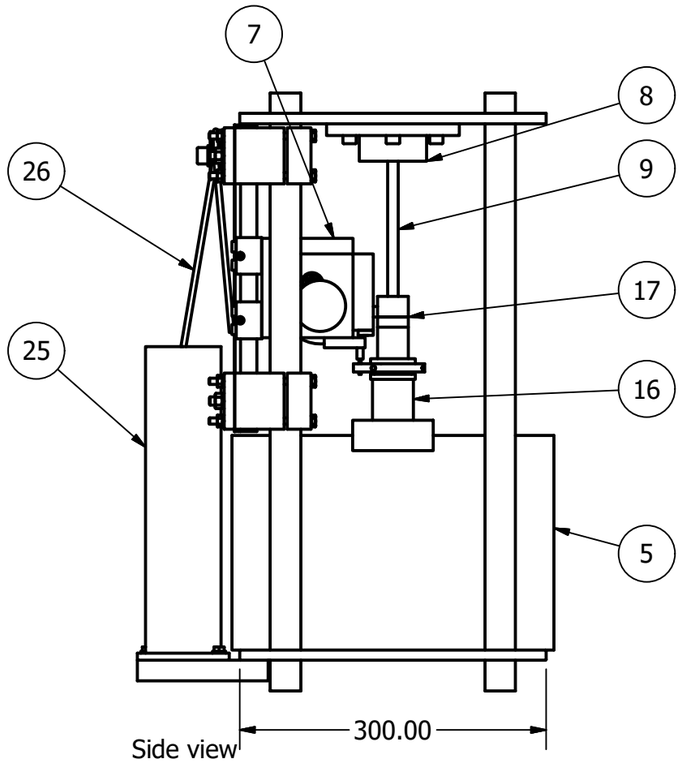

Side view

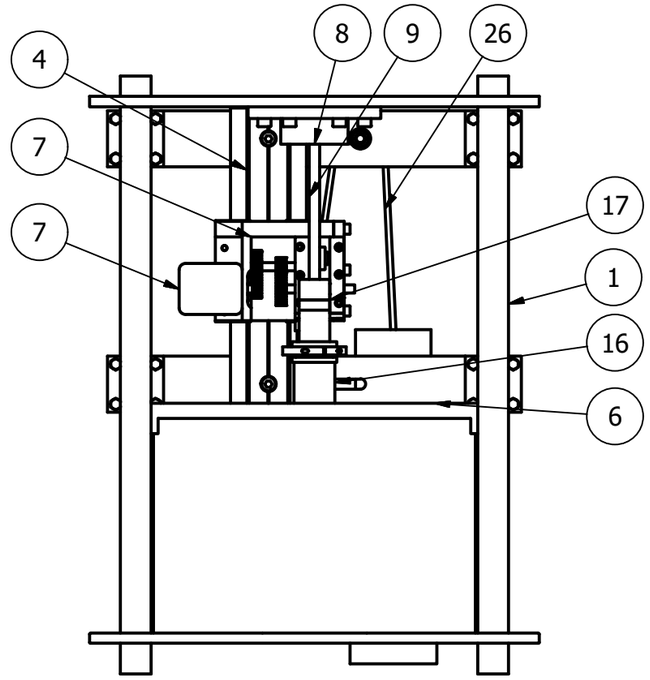

Front view

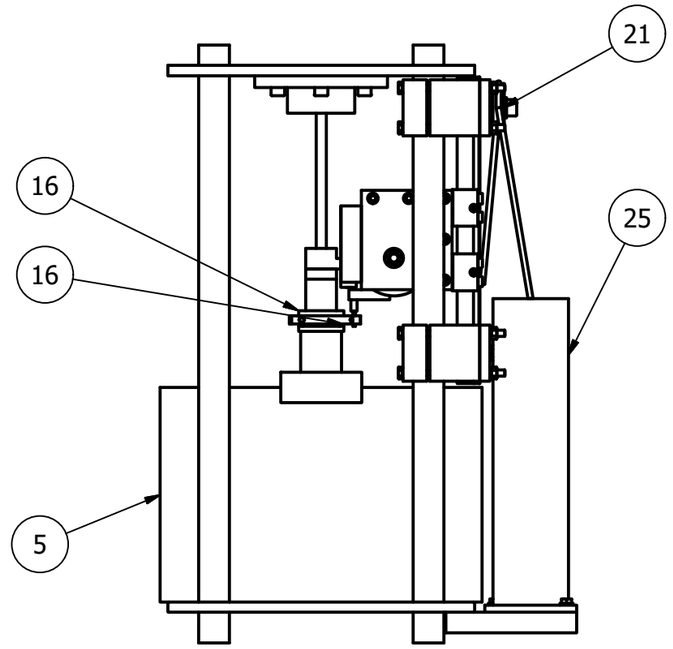

Side view

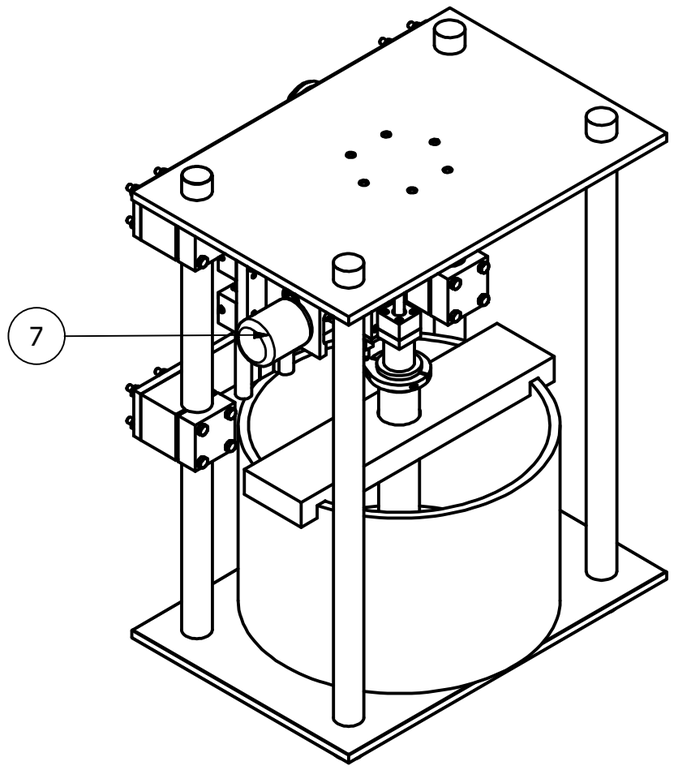

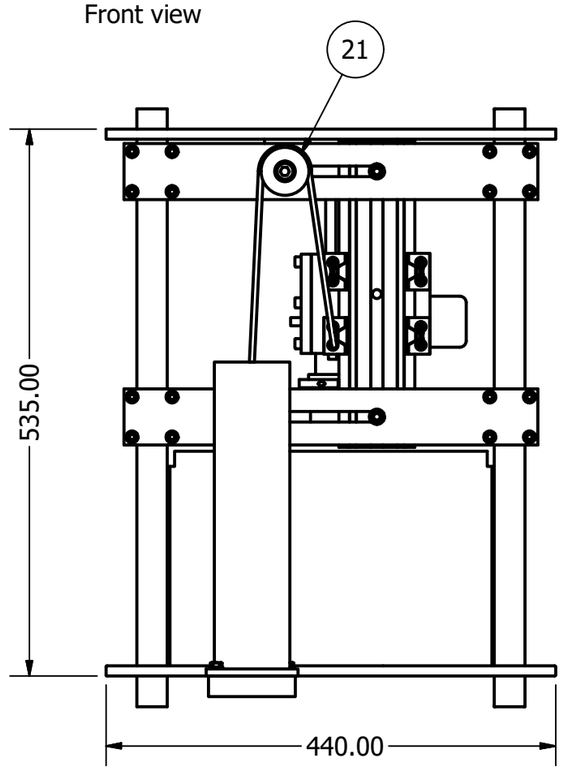

Back view

PARTS LIST	
ITEM	DESCRIPTION
1	Centrifuge carriage
4	Motor Guide rail
5	Strongbox
6	Pile guide
7	Motor housing
8	Guiding beam fixation
9	Ram mass guiding beam
16	Pile
17	Ram mass
21	Counterweight cable pulley
25	Counterweight housing
26	Counterweight cable

TU Delft, IHC MTI

TITLE

Overview Impact Pile driving hammer

SIZE	[mm]	Drawn
A3		J.C.B. van Zeben
SCALE 1/6		SHEET 1 OF 1

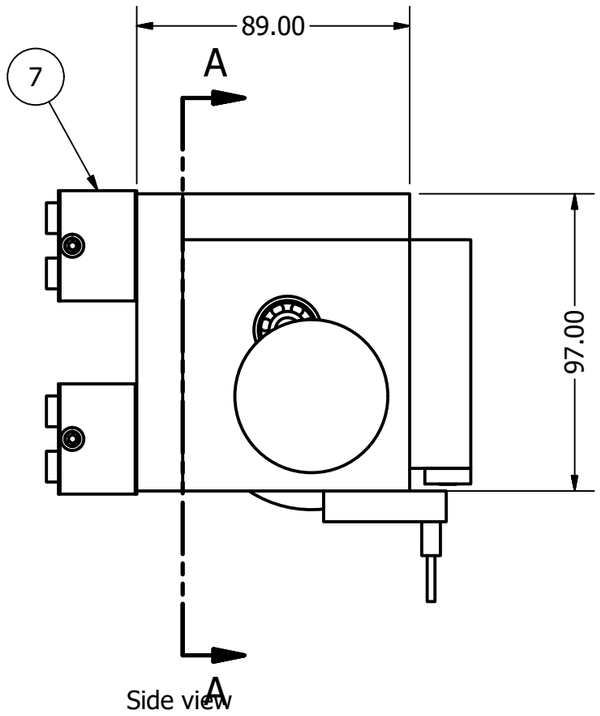

Side view

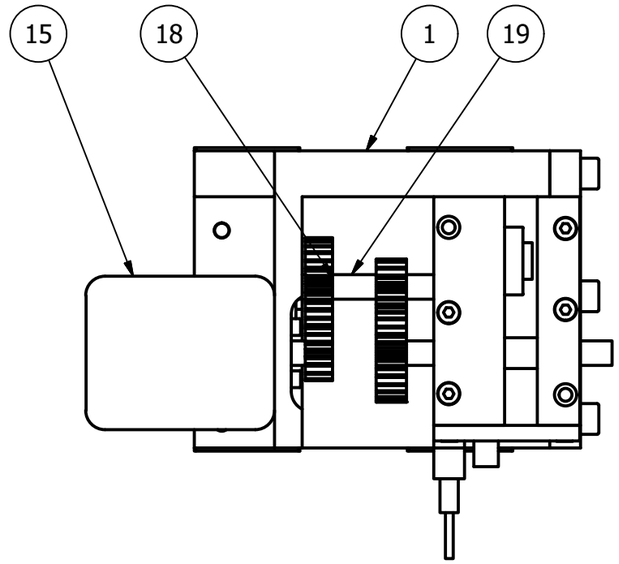

Front view

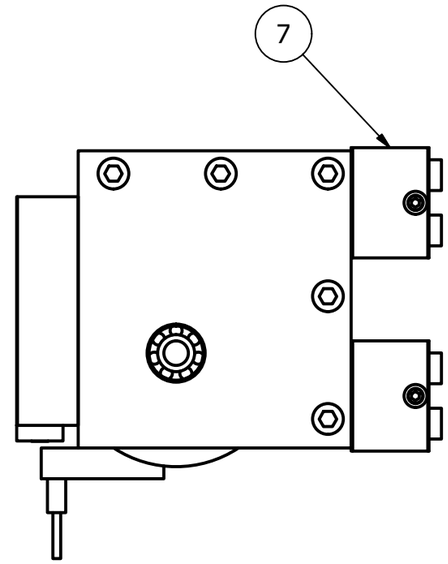

Side view

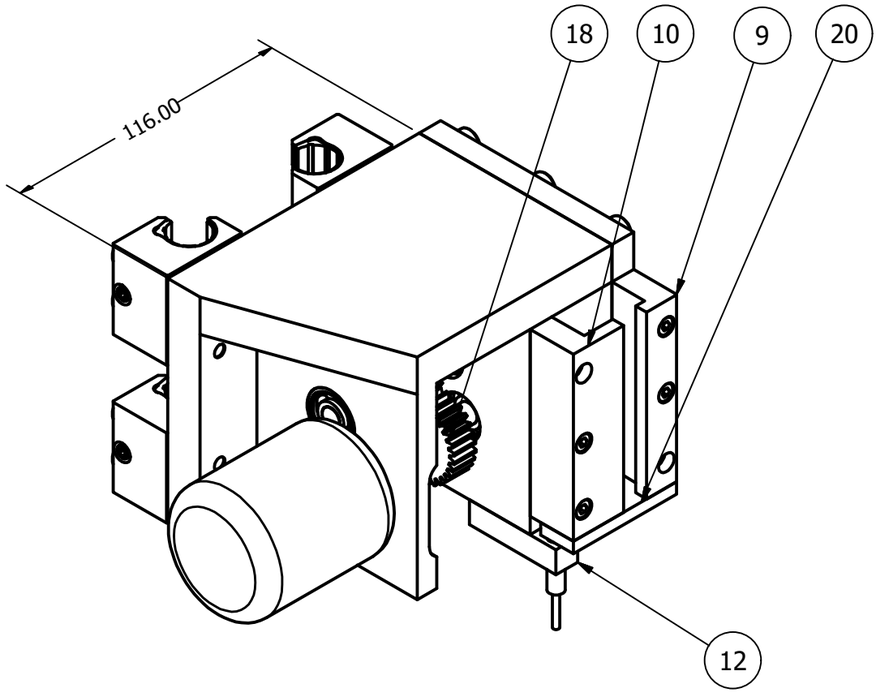

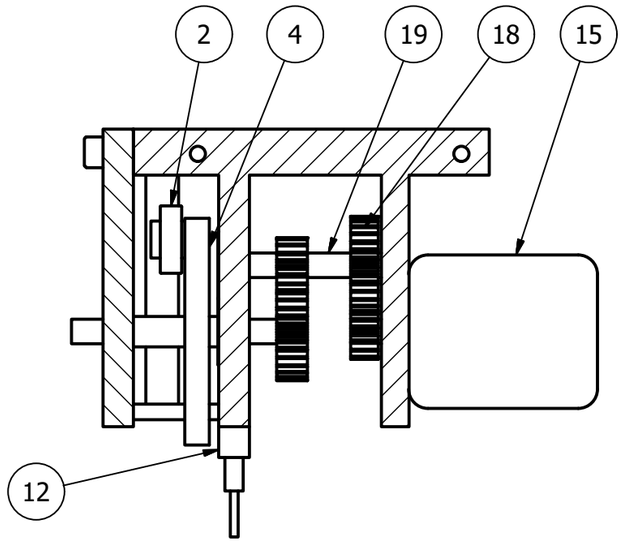

SECTION A-A

PARTS LIST	
ITEM	DESCRIPTION
1	Motor housing
2	Lift notch
4	Fly wheel
7	Linear guide block
9	Ram mass guiding rail
10	Ram mass guiding rail
12	Motor-pile connection
15	Electric motor
18	Gearbox
19	Gearbox axle
20	Ram mass stop bar

TU Delft, IHC MTI

TITLE

Pile driving hammer system

SIZE	[mm]	Drawn
A3		J.C.B. van Zeben
SCALE 1 / 2		SHEET 1 OF 1

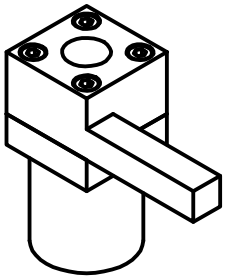

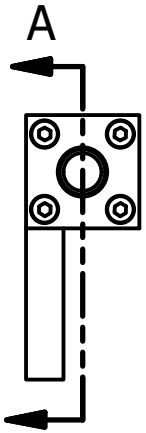

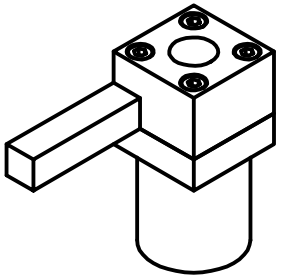

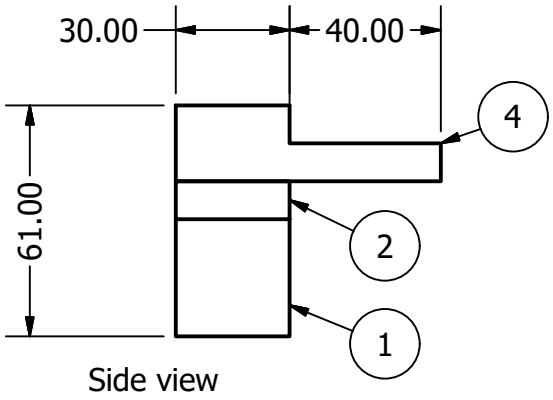

Side view

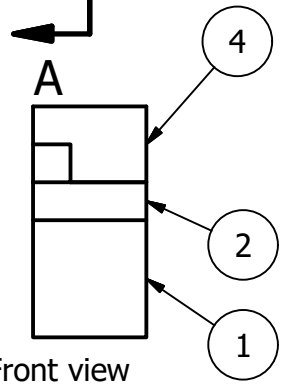

Front view

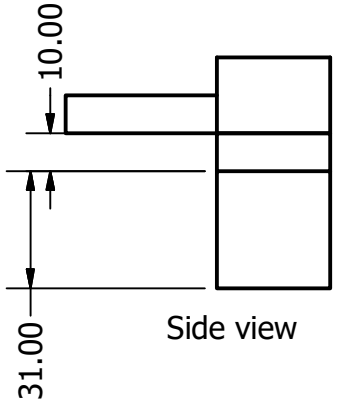

Side view

PARTS LIST	
ITEM	DESCRIPTION
1	Bearing house
2	Bearing house cap
3	Linear bearing
4	Top Cap

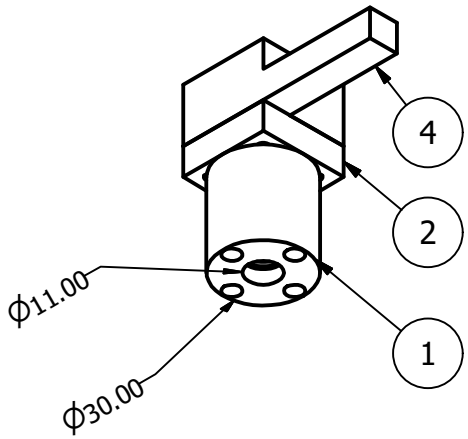

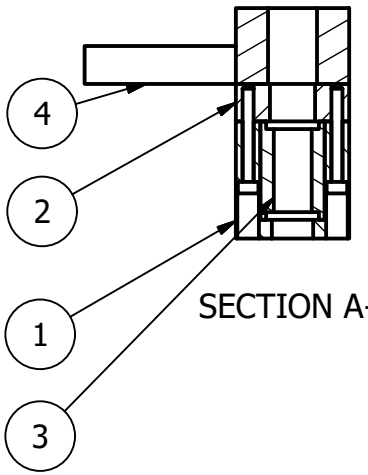

SECTION A-A

TU Delft, IHC MTI

TITLE

Ram mass

SIZE	[mm]	Drawn
A4		J.C.B. van Zeben
SCALE 1 / 2		SHEET 1 OF 1

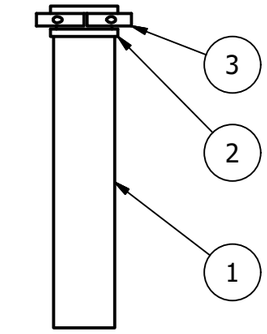

Side view

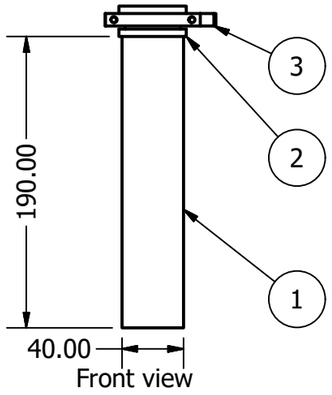

Front view

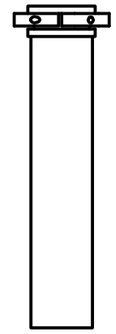

Side view

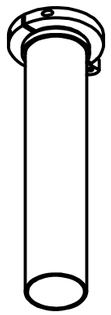

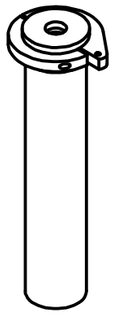

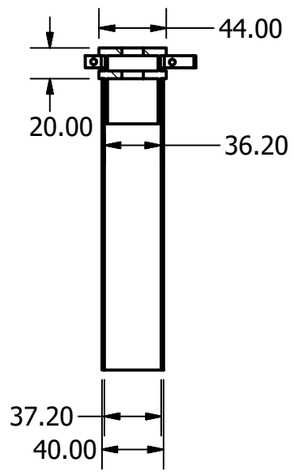

SECTION A-A

PARTS LIST	
ITEM	DESCRIPTION
1	Pile
2	Anvil
3	Clamping ring

TU Delft, IHC MTI

TITLE

Pile system

SIZE	[mm]	Drawn
A3		J.C.B. van Zeben
SCALE 1 / 4		SHEET 1 OF 1

Appendix C

Concept design Motor housing movement system

This document gives a concept design for improving the function of the impact pile driving hammer setup for the TU Delft centrifuge. The proposed design still needs detailing and especially the electronics part needs work. Kees van Beek from DEMO, Stevin lab II, should be consulted on both these aspects.

Concept design

The current impact pile driving setup is operational and can be used. During testing one aspect performed less than ideal. The motor housing that facilitates the lift of the ram mass is supposed to follow the pile as it is displaced. To achieve this the motor housing is situated on a guide rail and kept in balance by a counterweight and a spring. The concept behind this system is that the motor housing only exerts minimal downward force on the pile through the motor-pile connection. The counterweight counters most of the downward force while the spring ensures that as the motor housing goes down any effect from the gravity curve is countered. As the motor housing moves downward the g level working on it increases whilst the counterweight moves up and has less gravity effect.

In practice this system works less than ideal. The friction in the system is larger than expected. At the moment the motor housing weighs ca. 3.3 kg and the counterweight ca. 2.5 kg. Even with this weight difference downward movement is not ideal. Furthermore the spring is calibrated for 50g operations which means that if the motor housing is not in top position there is already significant tension in the spring. This pulls the motor housing upwards if a deeper pile embedment is used as a starting position. To mitigate this a concept design has been made to automatically lower the motor housing.

The basis of the improved design is an automated coupling between the measured pile displacement and the motor housing movement. The spring from the original design is taken away and the counterweight is reduced further to ca. 2 kg. This ensures the downward movement of the motor housing. To couple the movement from the pile to the motor housing a sailing winch servo is attached to counterweight cable. A sailing winch servo is capable of doing several rotations in contrast to a normal servo which has a position between 0 and 180 degrees. Because the counterweight is still in place the servo does not need to be very strong. Two pulleys are placed on an extra frame that can be attached to the back of the load frame. The sailing winch servo is attached to one of these pulleys. Over the pulleys a thin titanium fishing wire is placed. Since the counterweight is still in place the maximum pulling force that the servo needs to handle is ca. 50 kg. This does not require a large cable. The cable on the pulley system can be attached to the counterweight cable with a clamp. Depending on the rotation direction of the servo the motor housing now either goes up or down. The controller of pulley servo receives a direct feed from the pile displacement sensor. As the piles moves down the pulley servo moves the motor housing down a corresponding amount. See Figure 1 for a concept drawing.

In concept this design is promising but the following aspects need special attention when detailing.

- The signal from the pile displacement servo can have significant noise. This needs to be filtered before going to the pulley servo. If not properly filtered it will make the motor housing shake. This issue should be discussed with Kees van Beek.
- The total movement of the motor housing is ca. 120 mm. The amount of rotation needed from the servo is directly correlated to the diameter of the pulley. An optimization can be made between the required power from the servo and the diameter of the pulley.
- The pulley frame needs to be quite stiff as it probably needs to be hanged from only one loading frame bars.
- An alternative is to only allow downward movement. A single cable from the winch servo attached to the motor housing would then be needed. It would give less control over the setup.
- The proposed adaptation would negate the need of the motor-pile connection. Do not remove the motor-pile connection until the system has been extensively tested. If the motor moves down uncontrolled without this connection it will cause major damage.

- When further designing the system keep in mind that the entire motor housing weighs 1500 N.
- Servo's can be purchased at Quartell in Pijnacker. They are very knowledgeable and can help a lot. Show them the whole problem and they might give some good advice.

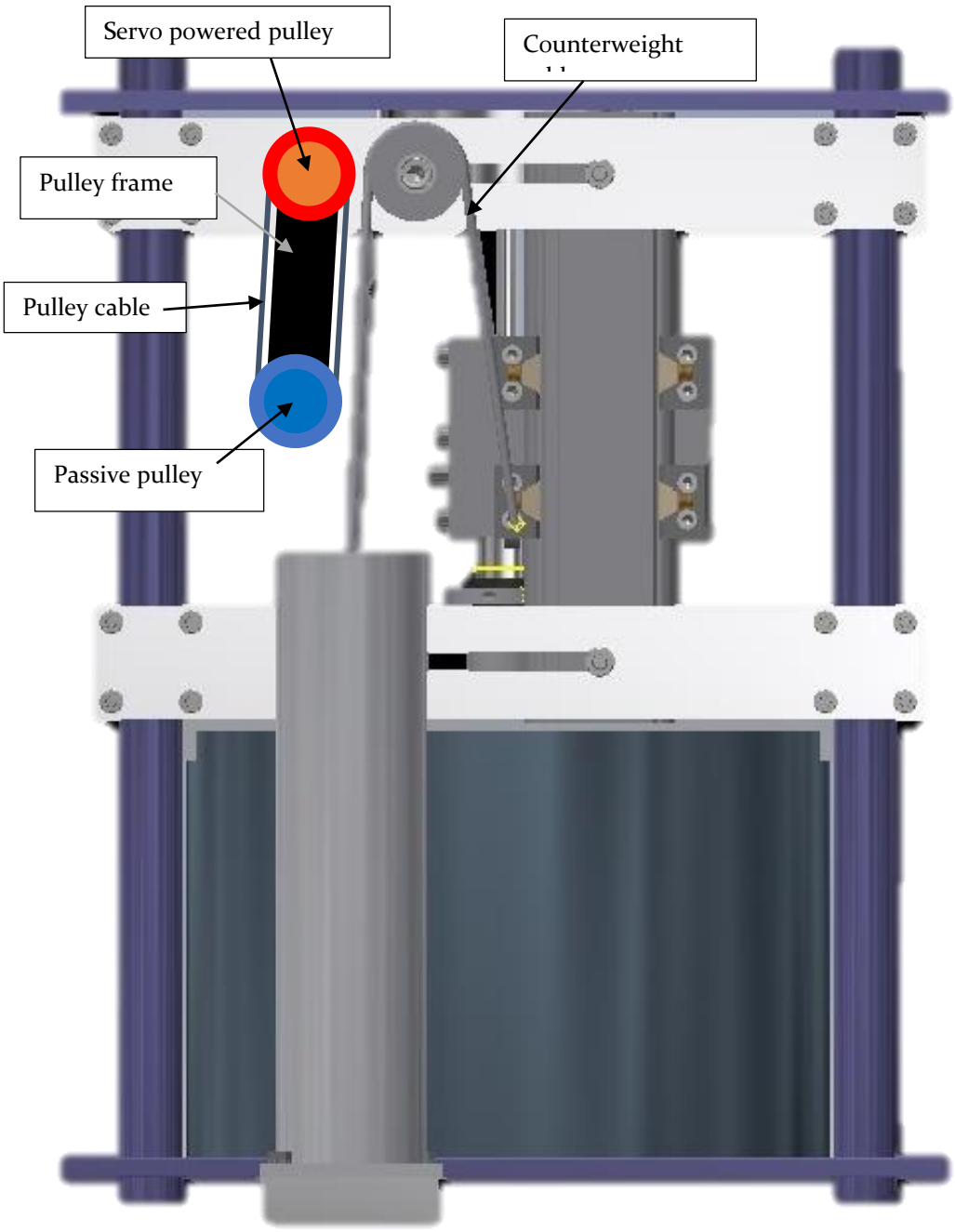

Figure 1 Concept design automated motor movement